



저작자표시-비영리-변경금지 2.0 대한민국

이용자는 아래의 조건을 따르는 경우에 한하여 자유롭게

- 이 저작물을 복제, 배포, 전송, 전시, 공연 및 방송할 수 있습니다.

다음과 같은 조건을 따라야 합니다:



저작자표시. 귀하는 원저작자를 표시하여야 합니다.



비영리. 귀하는 이 저작물을 영리 목적으로 이용할 수 없습니다.



변경금지. 귀하는 이 저작물을 개작, 변형 또는 가공할 수 없습니다.

- 귀하는, 이 저작물의 재이용이나 배포의 경우, 이 저작물에 적용된 이용허락조건을 명확하게 나타내어야 합니다.
- 저작권자로부터 별도의 허가를 받으면 이러한 조건들은 적용되지 않습니다.

저작권법에 따른 이용자의 권리는 위의 내용에 의하여 영향을 받지 않습니다.

이것은 [이용허락규약\(Legal Code\)](#)을 이해하기 쉽게 요약한 것입니다.

[Disclaimer](#)

A THESIS FOR THE DEGREE OF MASTER OF SCIENCE

**CO₂ Control Strategies for Sustainable Cultivation of
King Oyster Mushrooms and Romaine Lettuces in a
Closed Production System**

밀폐형 생산시스템 내 새송이 버섯과 로메인 상추의
지속적 재배를 위한 이산화탄소 제어 전략

BY

DAE HO JUNG

FEBRUARY, 2016

**MAJOR IN HORTICULTURAL SCIENCE AND
BIOTECHNOLOGY
DEPARTMENT OF PLANT SCIENCE
GRADUATE SCHOOL
COLLEGE OF AGRICULTURE AND LIFE SCIENCES
SEOUL NATIONAL UNIVERSITY**

**CO₂ Control Strategies for Sustainable Cultivation of
King Oyster Mushrooms and Romaine Lettuces in a
Closed Production System**

UNDER THE DIRECTION OF DR. JUNG EEK SON
SUBMITTED TO THE FACULTY OF THE GRADUATE SCHOOL OF SEOUL
NATIONAL UNIVERSITY

BY
DAE HO JUNG

DEPARTMENT OF PLANT SCIENCE
COLLEGE OF AGRICULTURE AND LIFE SCIENCES
SEOUL NATIONAL UNIVERSITY

FEBRUARY, 2016

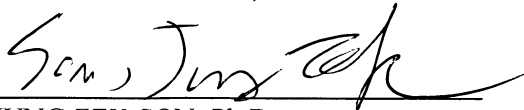
APPROVED AS A QUALIFIED THESIS OF DAE HO JUNG
FOR THE DEGREE OF MASTER OF SCIENCE
BY THE COMMITTEE MEMBERS

CHAIRMAN:



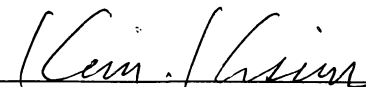
CHANGHOO CHUN, Ph.D

VICE-CHAIRMAN:



JUNG EEK SON, Ph.D

MEMBER:



KI SUN KIM, Ph.D

CO₂ Control Strategies for Sustainable Cultivation of King Oyster Mushrooms and Romaine Lettuces in a Closed Production System

Dae Ho Jung

Dept. of Plant Science, Graduate School of Seoul National University

ABSTRACT

Although the research of life support systems is getting active, it is difficult to perform actual experiments because various internal components in the system react complicatedly. Therefore modeling and simulation approaches have increased in the research of the life support system. A concept of supplying the CO₂ generated by mushrooms to lettuces by simultaneous cultivation is important in both of the life support system and crop production. The objectives of this study were to establish a CO₂ emission rate model for mushroom respiration, a photosynthetic rate model for lettuce photosynthesis, and to develop a simultaneous cultivation system of lettuce and mushroom. The CO₂ emission rate of mushrooms and photosynthetic rate of lettuces were measured using closed acrylic chambers. The coefficients of the models were statistically determined. By using the established models, the simultaneous cultivation system was constructed for lettuce and mushroom, and the CO₂ concentration in each chamber was predicted by simulation. And the difference between measured and estimated values was verified. R² values of the CO₂ emission and photosynthetic rate models were 0.64 and 0.94, respectively. The CO₂ concentrations in the simultaneous cultivation system were controlled within allowable

ranges. With the simultaneous cultivation system, CO₂ emission into the atmosphere could be reduced to 80.6% of the total CO₂ emitted from mushrooms by respiration. Based on this study, it is possible to control the CO₂ concentration for optimum cultivation, and to reduce the CO₂ emitted into the atmosphere during mushroom cultivation. Finally, it will help us to find out the appropriate gas circulation strategies in the life support system researches.

Additional key words: Closed cultivation system, CO₂ exchange, CO₂ model, Lettuce canopy photosynthesis, Mushroom respiration

Student Number: 2014-20016

CONTENTS

	Page
ABSTRACT	i
CONTENTS	iii
LIST OF TABLES	v
LIST OF FIGURES	vi
GENERAL INTRODUCTION	1
LITERATURE REVIEW	3
LITERATURE CITED	7
CHAPTER I. Estimation of CO ₂ Emission Rate of King Oyster Mushroom with Temperature and Growth Stage	11
Abstract	11
Introduction	12
Materials and Methods	14
Results	18
Discussion	20
Literature Cited	22

CHAPTER II. Estimation of Canopy Photosynthetic Rate of Heuk Romaine	35
Lettuce with CO ₂ Concentration and Growth Stage	
Abstract	35
Introduction	36
Materials and Methods	38
Results	41
Discussion	44
Literature Cited	45
CHAPTER III. Continuous Cultivation Strategies with CO ₂ Control for a Closed	56
Production of King Oyster Mushrooms and Romaine Lettuces	
Abstract	56
Introduction	57
Materials and Methods	59
Results and Discussion	62
Literature Cited	64
CONCLUSION	74
APPENDICES	75
ABSTRACT IN KOREAN	91

LIST OF TABLES

	Page
Table I-1. Parameters used in the models.	27
Table I-2. CO ₂ emission rate ($\mu\text{gCO}_2\cdot\text{s}^{-1}$) of the substrate according to temperature and growth period.	28
Table II-1. Parameters used in the models.	48
Table II-2. Regression results of photochemical efficiency, carboxylation conductance, dark respiration, and R ² values.	49
Table III-1. Parameters used in the models.	67
Table III-2. Photoperiod in the lettuce chambers.	68
Table III-3. Fresh weight and leaf area of the lettuces before and after experiments.	69

LIST OF FIGURES

	Page
Fig. I-1. Measurement of the CO ₂ emission rates of King Oyster mushrooms using a closed acrylic chamber in which the internal temperature was controlled within a range of 16-25°C.	29
Fig. I-2. Change in the mycelium proportion of King Oyster mushrooms as a function of days after scratching (DAS).	30
Fig. I-3. Change in the dry weight of King Oyster mushroom sporophores as a function of days after scratching (DAS).	31
Fig. I-4. Quadratic equation regression results of the maintenance (A) and CO ₂ production (B) coefficients as a function of temperature before and after thinning.	32
Fig. I-5. Three-dimensional diagram of the CO ₂ emission rates of King Oyster mushroom cultivation bottles according to temperature and days after scratching (DAS).	33
Fig. I-6. Validation of the estimated and measured CO ₂ emission rates in King Oyster mushroom cultivation bottles.	34
Fig. II-1. Measured shoot fresh and dry weights, and leaf area of the lettuce with growth stage.	50
Fig. II-2. Relationship between atmospheric (C_a) and intercellular (C_i) CO ₂ concentrations in the lettuce leaves.	51

Fig. II-3. Regressed A/Ci curves at difference growth stages of DAT 4, 7, 14, 21 and 28.	52
Fig. II-4. Regressed results of photochemical efficiency, carboxylation conductance, and dark respiration.	53
Fig. II-5. Regressed results of the simple multiplication model (A) and Thornley model (B) of canopy photosynthetic rates according to intercellular CO ₂ concentration and growth stage.	54
Fig. II-6. Validation of canopy photosynthetic rates of the simple multiplication model and Thornley model.	55
Fig. III-1. Conceptual diagram of a system consisting of three lettuce chambers, one mushroom chamber, and one CO ₂ mixing chamber.	70
Fig. III-2. Schematic diagram of the continuous cultivation.	71
Fig. III-3. Actual and simulated CO ₂ concentrations in each chamber for 3 days; lettuce chamber 1 (A), lettuce chamber 2 (B), lettuce chamber 3 (C), mushroom chamber (D), and mixing chamber (E).	72
Fig. III-4. Accumulated CO ₂ emission into the atmosphere for 3 days.	73

GENERAL INTRODUCTION

Entering the 21st century, development of science and technology has been rapidly growing with an exponential increase of population, and many impossible things have become possible. However human beings are still not satisfied and trying to find something new. As a result, the interest in science fiction (SF) is getting hotter day by day. SF has been expressed as various formats, such as movie. *Sunshine* (2007), *Snowpiercer* (2013), *Gravity* (2013), *Interstellar* (2014), and *Martian* (2015) released in 10 years are good examples of the SF movies. Peoples appeared in the films want to go where cannot go or want to live where cannot survive. The films showed detail apparatus enable them alive. For example, in the *Sunshine* oxygen generated from the garden is supplied to the crew and a certain train compartment grows plants in the *Snowpiercer*.

The life support system can be divided largely into three parts of open-, semi-closed- and closed-loop systems according to the path and movement of resources. The open-loop system has an advantage that can be easily used to create, but a disadvantage in poor efficiency of long-term missions. The closed-loop system has a good efficiency in the long-term missions, but complex interactions among internal components (Barta and Henninger, 1994; Eckart, 1996). The regeneration techniques used in the closed-loop way include the physio-chemical regeneration and biological regeneration methods (Shaw, 2014). The biological regeneration method has been studied in some experiments such as Biosphere 2. It is considered as the only way that a massive ecosystem can be maintained over a long period of time (Nelson et al., 1994).

However, the actual design of closed-loop life support systems has many difficulties in demands of a lot of money for large-scale experimental equipment and biomasses as well as a long time to design. Therefore modeling and simulation techniques can be a good solution. Through creating a model for an actual system, expressing the physical phenomenon by mathematical form, and obtaining a hermeneutical solution by simulation, it is possible to derive the results of the experiments which are difficult to perform actually (Sokolowski and Banks, 2010).

Production and consumption of the CO₂ as elements in the life support system are suitable for the researches utilizing modeling and simulation techniques. There was an attempt to supply the CO₂ generated during mushroom cultivation to the lettuce cultivation (Kitaya et al., 1994). However, in this study, the amounts of CO₂ emitted by mushroom respiration and consumed by lettuce photosynthesis were not quantified. For efficient management of total cultivation system for mushrooms and lettuces, it is necessary to quantify and to establish the models of the CO₂ emission by mushrooms and consumed by lettuces.

The objectives of this study were to establish a CO₂ emission rate model for mushroom respiration and a CO₂ consumption rate model for lettuce photosynthesis, compare the actual and estimated CO₂ concentrations in the mushroom and lettuce chambers, and to develop a simultaneous cultivation system of lettuce and mushroom.

LITERATURE REVIEW

Mushroom Respiration Model

In mushroom cultivation, CO₂ is emitted during sporophore initiation, and mycelium and sporophore growth. The amount of CO₂ emitted depends on the specific strain, weight and moisture content of the medium, incubation temperature, and growth period (Jang et al., 2007). Zdražil (1975) reported that the mycelium growth of *Pleurotus* mushrooms is suppressed when exposed to high CO₂ concentrations of 22-28%. In addition, the expansion of sporophore pileus is inhibited at a CO₂ concentration of 3,000-9,000 μmol·mol⁻¹ (Kinugawa et al., 1994), while the best quality of the mushroom sporophores are optimal at 2,400 μmol·mol⁻¹ (Ryu et al., 2005).

There are existing mathematical models used to express the separate growth of medium and mycelium and sporophore mushroom parts. Likewise, the respiration rate of each of these parts can be represented using dry weight models of the mycelium and sporophores (Chanter and Thornley, 1978). The rates of respiration of the mycelium and sporophores can be derived from the respiration model developed by Thornley (1970).

$$R = M * W + P * \frac{dW}{dt}$$

where R is the CO₂ emission rate or respiration rate, W is the dry weight of mushroom, M is the maintenance coefficient, and P is the CO₂ production coefficient. And the mathematical model for mycelial growth and the initiation and growth of sporophores in

the mushroom crop is extended to allow for harvesting of the sporophores (Chanter, 1979). The model is used to demonstrate the importance of using regular harvesting schedules in mushroom cropping experiments.

Yang et al. (2011) reported that the effect of different temperature and humidity on mycelium growth was analyzed by using the GIS data acquisition tools. It is considered that the optimal temperature and relative humidity conditions for King Oyster mushroom growth were 16°C and 95%.

Plant Photosynthesis Model

Explanatory models allow for testing hypotheses and synthesizing knowledge and facilitate comprehension of complex systems. Most explanatory models are photosynthesis based models (Marcelis et al., 1998). For leaves the light response curve of gross photosynthesis can be generalized to:

$$P_g = P_{g,max} \times f(x)$$

where $P_{g,max}$ is the maximum rate of leaf photosynthesis and x is the dimensionless parameter. To represent the function $f(x)$, one of the most general functions that express the photosynthesis is the non-rectangular hyperbola:

$$f(x) = \frac{1 + x - \sqrt{(1 + x)^2 - 4x\theta}}{2\theta}$$

where parameter θ regulates the shape of this function.

In the biochemical approach of Farquhar et al. (1980) the photosynthetic properties of the leaf are expressed in the basic characteristics of Rubisco enzyme kinetics and electron

transport capacity. This approach can be allowed for description of the temperature and CO₂ dependence of photosynthesis. Thus, the FvCB model is consisted of Rubisco limited part and RuBP regeneration limited part:

$$A = \begin{cases} V_{max} \frac{C_c - \Gamma^*}{K_c \left(1 + \frac{O}{K_o}\right) + C_c} - R_d : \text{Rubisco limited} \\ \frac{J}{4} \frac{C_c - \Gamma^*}{C_c + 2\Gamma^*} - R_d : \text{RuBP regeneration limited} \end{cases}$$

where, V_{max} is the Rubisco activity, Γ^* is the CO₂ compensation point in the absence of dark respiration, K_c is the Michaelis-Menten constant for carboxylation by Rubisco, O is the partial pressure of oxygen within the chloroplast, K_o is the Michaelis-Menten constant for oxygenation by Rubisco, R_d is the rate of dark respiration in the light and J is the rate of electron transport.

However, in order to measure the canopy photosynthetic rate, the closed types of chamber are mainly used. The closed type chambers have a difficulty in measuring the steady state photosynthesis (Bugbee, 1992). Thus, the dynamic model for photosynthesis is required to express the canopy photosynthesis. Perhaps the equation that is most commonly used to describe steady-state photosynthetic response to light and CO₂ is the rectangular hyperbola:

$$P_g = \frac{\alpha I \beta C}{\alpha I + \beta C}$$

where P_g is the steady-state photosynthetic rate, I is the light-flux density, C is the CO₂ concentration and α and β are constants. However, the equation above can be modified through the solving simple differential equations to be used in the situation in which the

light fluctuation and CO₂ fluctuation (Kaitala et al. 1982; Thornley, 1974).

Life Support Systems

Astronauts are surrounded by the hostile environment of space. Only the life support system is dedicated explicitly to the survival of the crew. Complicated interactions exist between a lot of life support system technologies and components (Hendrickx et al., 2006; Volk and Rummel, 1987).

The life support system can be divided largely into three parts according to the path and movement of resources. There is an open-loop way that consumed resources by crew and discharged to waste, and a closed-loop way that regenerates all the resources to reuse. And a semi-closed-loop way is a compromise between the open-and closed-loop ways. The open-loop system has an advantage that can be easily used to create, but a disadvantage in poor efficiency of long-term missions. The closed-loop system has a good efficiency in the long-term missions, but complex interactions among internal components (Barta and Henninger, 1994; Eckart, 1996).

According to the Environmental Controlled Life Support System (ECLSS) roadmap released by NASA, the regeneration techniques used in the closed-loop way include the physio-chemical regeneration and biological regeneration methods (Metcalf et al., 2011). Shaw (2014) summarized that all the life support system can be classified systematically depending on the resources regeneration methods. The physicochemical regeneration life support system has a characteristic that relies on physical or chemical processes to transform or relocate resources. It mainly used in relatively short term space missions or

situations that easily supplied. On the other hand, the biological regeneration life support system has a characteristic that relies on biological processes to transform resources. In this case, living organism such as plant, bacteria or others are actively and intentionally used for the regeneration of the resources. The Earth is an entire biological regeneration life support system.

Biological regeneration method has been studied in some experiments such as Biosphere 2. It is considered as the only way that a massive ecosystem can be maintained over a long period of time (Nelson et al., 1994). Biological regenerative technologies developed by the Biosphere 2 project may find applications in the initial and near-term life support systems. Recently, the Virtual Habitat Project (V-HAB) was initialized to develop an engineering tool allowing dynamic simulations of different life support system architectures, enabling optimization of the life support system design in early stages of development (Olthoff et al., 2014). V-HAB project contains the plant model based on modified energy cascade model. The plant model consisted of two plant chambers; one containing wheat, soybean, potato and rice cultures and the other containing lettuce and beet.

LITERATURE CITED

Barta, D.J., and D.L. Henninger. 1994. Regenerative life support systems – why do we need them? *Advances in Space Research*. 14: 403-410.

- Bugbee, B. 1992. Steady-state canopy gas exchange: system design and operation. *HortScience* 27: 770-776.
- Cannell, M.G.R., and J.H.M. Thornley. 2000. Modelling the components of plant respiration: Some guiding principles. *Annals of Botany* 85: 45-54.
- Chanter, D.O. 1979. Harvesting the mushroom crop: a mathematical model. *Journal of General Microbiology* 115: 79-87.
- Chanter, D.O., and J.H.M. Thornley. 1978. Mycelial growth and the initiation and growth of sporophores in the mushroom crop: a mathematical model. *Journal of General Microbiology* 106: 55-65.
- Eckart, P. 1996. *Spaceflight life support and biospherics*. Kluwer Academic Publishers, pp. 80-81.
- Farquhar, G.D., S. von Caemmerer, and J.A. Berry. A biochemical model of photosynthetic CO₂ assimilation in leaves of C₃ species. *Planta* 149: 78-90.
- Hendrickx, L., H. de Wever, V. Hermans, F. Mastroleo, N. Morin, A. Wilmotte, P. Janssen, and M. Mergeay. 2006. Microbial ecology of the closed artificial ecosystem MELiSSA (Micro-Ecological Life Support System Alternative): Reinventing and compartmentalizing the Earth's food and oxygen regeneration system for long-haul space exploration missions. *Research in Microbiology*. 157: 77-86.
- Jang, M.J., T.M. Ha, and Y.C. Ju. 2007. Comparison of respiration characteristics on the new variety of oyster mushroom according to the growth temperature. *Journal of Mushroom Science and Production* 5: 65-70.

- Kaitala, V., P. Hari, E. Vapaavuori, and R. Salminen. 1982. A dynamic model for photosynthesis. *Annals of Botany* 50: 385-396.
- Kinugawa, K., A. Suzuki, Y. Takamatsu, M. Kato, and K. Tanaka. 1994. Effects of concentrated carbon dioxide on the fruiting of several cultivated basidiomycetes (II). *Mycoscience* 35: 345-352.
- Kitaya, Y., A. Tani, M. Kiyota, and I. Aiga. 1994. Plant growth and gas balance in a plant and mushroom cultivation system. *Advanced Space Research* 14: 281-284.
- Marcelis, L.F.M., E. Heuvelink, and J. Goudriaan. 1998. Modelling biomass production and yield of horticultural crops: a review. *Scientia Horticulturae* 74: 83-111.
- Metcalf, J., R. Carrasquillo, L. Peterson, B. Bagdigian, and D. Westheimer. 2011. Environmental control and life support (ECLS) integrated roadmap development. National Aeronautics and Space Administration Technical Report, Huston, Texas.
- Nelson, M., W. Dempster, N. Alvarez-Romo, and T. MacCallum. 1994. Atmospheric dynamics and bioregenerative technologies in a soil-based ecological life support system: initial results from biosphere 2. *Advances in Space Research*. 14: 417-426.
- Olthoff, C., J. Schnaitmann, and A. Zhukov. 2014. Development status of the dynamic life support system simulation V-HAB. 44th International Conference on Environmental Systems, Tucson, Arizona.
- Ryu, J.S., M.K. Kim, S.H. Cho, Y.C. Yun, W.M. Seo, and H.S. Lee. 2005. Optimal CO₂ level for cultivation of *Pleurotus eryngii*. *Journal of Mushroom Science and Production* 3: 95-99.

- Shaw, M.M. 2014. An analysis of hybrid life support systems for sustainable habitats. MS Thesis. Massachusetts Institute of Technology.
- Sokolowski, J.A., and C.M. Banks. 2010. Modeling and simulation fundamentals: theoretical underpinnings and practical domains. John Wiley & Sons, New Jersey, USA. pp. 2-4.
- Thornley, J.H.M. 1970. Respiration, growth and maintenance in plants. *Nature* 227: 304-305.
- Thornley, J.H.M. 1974. Light fluctuations and photosynthesis. *Annals of Botany* 38: 363-373.
- Volk, T., and J. D. Rummel. 1987. Mass balances for a biological life support system simulation model. *Advances in Space Research*. 7: 141-148.
- Yang, J., J.Y. Zhao, Q. Guo, Y.S. Wang, and R.J. Wang. 2011. Data acquisition method for measuring mycelium growth of microorganism with GIS. *Computer and Computing Technologies in Agriculture IV*. Springer. pp. 374-380.
- Zadrazil, F. 1975. Influence of CO₂ concentration on the mycelium growth of three *pleurotus* species. *European Journal of Applied Microbiology and Biotechnology* 1: 327-335.

CHAPTER I

Estimation of CO₂ Emission Rate of King Oyster Mushroom with Temperature and Growth Stage

ABSTRACT

Temperature and CO₂ are important controllable factors in mushroom cultivation. CO₂ is produced during mushroom respiration, and accumulation of high concentrations of CO₂ can induce specific disorders in the fungi. The objective of this study was to quantify the CO₂ emission rate of King Oyster mushrooms (*Pleurotus eryngii* (DC.) Quél) as a function of temperature and growth stage. The CO₂ emission rates of the substrate and sporophores were separately measured in closed acrylic chambers (1.0m x 0.8m x 0.5m) at 8, 12, and 15 days after scratching at temperatures of 16°C, 18°C, 20°C, 22°C, and 25°C. Regression analysis was performed using the measured CO₂ emission rates to obtain respiration models. Finally, CO₂ emission rate models consisting of the substrate and sporophores were developed for the growth periods before and after thinning. The CO₂ emission rates estimated by the model were compared with the actual rates and showed an agreement of $R^2 = 0.642$. Finally, using the established model, the optimal CO₂ conditions for mushroom growth were obtained.

Additional key words: Model, Respiration, Sporophore, Substrate, Thinning

INTRODUCTION

Commercial cultivation of mushrooms has increased sharply over the last few decades with the development of cultivation techniques. Among mushrooms such as *Agaricus*, *Lentinus*, *Pleurotus*, *Auricularia*, *Volcariella*, *Flammulina*, and *Tremella* (Kües and Liu, 2000), Oyster mushrooms (*Pleurotus* genus) are widely cultivated in East Asia regions. The bottle cultivation methods developed since the 1950s have enabled large-scale production for commercial purposes (Iwase, 1997; Kües and Liu, 2000; Yamanaka, 2011). However, because King Oyster mushrooms (*P. eryngii*) are typically cultivated in bottles, adequate control of environmental factors such as temperature, humidity, and CO₂ concentration is required (Lee et al., 2003).

In mushroom cultivation, CO₂ is emitted during mycelium growth, sporophore initiation, and sporophore growth. The amount of CO₂ emitted depends on the specific strain, weight and moisture content of the medium, incubation temperature, and growth period (Jang et al., 2007). Mycelium growth and sporophore quality are negatively affected by accumulation of CO₂. Indeed, Zdražil (1975) reported that the mycelium growth of *Pleurotus* mushrooms is suppressed when exposed to high CO₂ concentrations of 22-28%. In addition, the expansion of sporophore pileus is inhibited at CO₂ concentrations of 3,000-9,000 $\mu\text{mol}\cdot\text{mol}^{-1}$ (Kinugawa et al., 1994), while the quality of the mushroom is optimal at 2,400 $\mu\text{mol}\cdot\text{mol}^{-1}$ (Ryu et al., 2005). To prevent physiological disorders during mycelium growth and sporophore formation in high CO₂ concentrations, levels should be adequately

controlled (Jang et al., 2007; Jang et al., 2009; Ryu et al., 2005). Quantitative analysis of mushroom CO₂ emissions is thus very important, although it has been rarely performed.

There are existing mathematical models used to express the separate growth of medium and mycelium and sporophore mushroom parts. Likewise, the respiration rate of each of these parts can be represented using dry weight models of the mycelium and sporophores (Chanter and Thornley, 1978). However, it is difficult to separate the medium from the mycelium under conditions of bottle cultivation. Thus, in order to establish the CO₂ emission rate model of the mushroom, it is necessary to determine the amount of mycelium in the substrate and use growth models reflecting the growth characteristics of sporophores. In order to estimate the mycelium abundance, an image processing method utilizing photographs of sections of medium was developed, in which the percentage change in mycelium as a function of temperature and humidity is expressed by a quadratic equation model (Yang et al., 2012). However, it is not possible to determine the change in respiration rate of different mushroom parts according to environmental conditions using existing models.

Repeated harvesting of sporophores from medium may reduce the number and weight of sporophores (Burton and Noble, 1993; Flegg and Smith, 1982). For practical purposes, a method involving cutting all but 1-2 large sporophores, called thinning, is widely used to improve the quality of King Oyster mushroom cultivars (Ryu et al., 2005). Therefore, models of the CO₂ emission rate of sporophores should include the thinning process. The objectives of this study were to separately measure the CO₂ emission rates of substrate and

sporophore and to establish a CO₂ emission rate model of mushrooms as a function of temperature and growth stage.

MATERIALS AND METHODS

Incubation and Growth Conditions of Mushrooms

King Oyster mushrooms (*Pleurotus eryngii* (DC.) Quél) cultivated in Ain-Farm (Geumgwangmyeon, Anseong, Korea) were used in this study. The disclosure strain was Sae song-ee No. 2, developed by Gyeonggi Agricultural Research Institute, Korea. The substrate used for mushrooms consisted of a 1:1:2 mixture of sawdust:corn cob:additive with a water content of 65-68%. The additives included beet pulp, soybean meal, wheat bran, and dried bean curd. For cultivation, 950 mL polypropylene bottles were filled with 570 g of substrate and sterilized for 60-90 min at 121°C. Inoculated mycelia were incubated for 26-28 days and post-incubated for 5 or 6 days in an incubation room maintained at a temperature of 21-22°C and relative humidity of 65-70%. After scratching, the temperature and relative humidity in the incubation room were gradually changed from 18 to 15°C and from 95 to 80-85%, respectively.

Measurement of the Mycelium Ratio in Bottles according to Growth Stage

In order to analyze the growth of mycelium and sporophore according to days after scratching (DAS), fresh and dry weights of mycelium and substrate were measured at DAS 8, 12, and 15. To estimate the percentage of mycelium in the substrate, photographs of five cross-sections of cylindrical bottles (at 2 cm intervals) were taken in three replications. Photographs were converted to binary images using Image J (US National Institutes of Health, Bethesda, MD, USA), and the ratios corresponding to the percentages of substrate and mycelium were obtained by calculating the number of pixels.

Measurement of CO₂ Emission Rate of Substrate and Sporophores according to Temperature and Growth Stage

To measure the CO₂ emission rates of substrate and sporophores, mushrooms were placed in closed acrylic chambers (1.0 m × 0.8 m × 0.5 m) maintained at a constant internal temperature (Fig. 1). CO₂ concentrations were measured using an infrared CO₂ sensor (LI-820, LI-COR, Lincoln, NE, USA) controlled by a data logger (CR1000, Campbell Scientific, Logan, UT, USA). Mushrooms at DAS 8, 12, and 15 were used for measurement of CO₂ emission rates. At DAS 12, all but the two largest sporophores of 2.5 to 3 cm were removed. Three mushroom bottles corresponding to each growth period were then placed in the chamber, and the CO₂ emission rates were measured in triplicate. The CO₂ emission rate of a single mushroom bottle was calculated by measuring the CO₂ concentration in the closed chamber every 5 sec. After removing sporophores, the CO₂ emission rate of the substrate was measured again using the same method. The CO₂ emission rates of the

mushrooms at DAS 8, 12, and 15 were measured at temperatures of 16°C, 18°C, 20°C, 22°C, and 25°C.

CO₂ Emission Models of the Substrate and Sporophore according to Temperature and Growth Stage

To establish a CO₂ emission model of the mushrooms, the measured CO₂ emission rates were regressed using the statistical program SPSS (SPSS Inc., Chicago, IL, USA). The CO₂ emission rate of the substrate as a function of temperature was expressed using Eq. I-1. The symbols used in the models are summarized in Table I-1.

$$R_m = a_1 * T^2 + a_2 * T + a_3 \quad \text{Eq. I-1}$$

Regression analysis was conducted at DAS 8 before thinning and at DAS 12 and 15 after thinning.

Although sporophore growth is known to follow the Gompertz equation (Chanter and Thornley, 1978), the sporophores of King Oyster mushroom in this study were harvested before reaching the stationary phase and were thus evaluated using an exponential function (Fig. I-2). Specifically, when the relative growth rate k is assumed to be constant after thinning, it is possible to express sporophore growth by substituting W_0 for W_T as follows.

$$W_s = W * e^{k*t} \quad \text{Eq. I-2}$$

Using the measured dry weights of the sporophores at DAS 8, 9, 11, 12, 13, and 15, regression analysis was performed with respect to time t .

The respiration rate of sporophores, divided into growth respiration and maintenance respiration, was determined by Eq. I-3, which consists of the dry weight and its rate of change (Cannell and Thornley, 2000; Chanter and Thornley, 1978; Thornley, 1970). By substituting Eq. I-2 into Eq. I-3, the following model of sporophore respiration was obtained (Eq. I-4).

$$R = M * W + P * \frac{dW}{dt} \quad \text{Eq. I-3}$$

$$R_s = M * W * e^{k*t} + P * W * k * e^{k*t} \quad \text{Eq. I-4}$$

The maintenance coefficient and CO₂ production coefficient in Eq. I-4 were defined as follows:

$$M = a_4 * T^2 + a_5 * T + a_6 \quad \text{Eq. I-5}$$

$$P = a_7 * T^2 + a_8 * T + a_9 \quad \text{Eq. I-6}$$

The regression coefficients in Eqs. I-5 and I-6 were determined using the measured CO₂ emission rates of the sporophores substituted into Eq. I-4. The model was expressed using two variable equations that included the growth period and temperature.

Validation of the CO₂ Emission Model

At DAS 7, 9, 11, 13, and 15, the CO₂ emission rates of the bottle-cultivated mushrooms at a temperature of 24°C were measured in the closed chamber. The model was validated using linear regression analysis by comparing the measured CO₂ emission rates and those estimated from the model.

RESULTS

Mycelium Ratio and CO₂ Emission Rate of the Substrate with Growth Stage

The mycelium ratio of the substrate was 28.01±3.64%, 27.23±2.62%, and 32.08±3.91% at DAS 8, 12, and 15, respectively, and showed no significant difference as a function of time (Fig. I-2). Conversely, the CO₂ emission rates of the substrate before and after thinning were significantly different (Table I-2). Using the parameters in Eq. I-1, obtained by regression analysis, the CO₂ emission rates of the substrate before and after thinning were described using Eqs. I-7 and I-8, respectively. The value of R² in both cases was approximately 0.79, indicating the high reliability of the models.

$$R_{mb} = -1.313 * 10^{-5} * T^2 + 2.412 * T + 0.117 \quad \text{Eq. I-7}$$

$$R_{ma} = 0.027 * T^2 + 5.108 * T - 30.732 \quad \text{Eq. I-8}$$

Growth and CO₂ Emission Rate of Sporophores

The dry weight of the sporophores increased exponentially with time (Fig. I-3). The initial dry weight of sporophores before thinning (W_0) was 0.009 g, and the relative growth rate k according to Eq. I-2 was 0.549. The initial dry weight of sporophores after thinning (W_T) was 0.002, which was which obtained from Eq. I-2 using regression analysis. The value of R² in the two cases was estimated as 0.790 and 0.881, respectively. The CO₂ emission rates of the sporophores before and after thinning in Eq. I-4 were described using Eqs. I-9 and I-10, respectively.

$$R_{sb} = (0.009 * M_b * +0.00494 * P_b) * e^{0.549*t} \quad \text{Eq. I-9}$$

$$R_{sa} = (0.002 * M_a * +0.00110 * P_a) * e^{0.549*t} \quad \text{Eq. I-10}$$

Using the regression analysis with temperature, the values of M_b , M_a , P_b , and P_a were derived (Fig. I-4).

Total CO₂ Emission Rate of One Bottle of King Oyster Mushroom

The CO₂ emission rate models for a mushroom cultivation bottle before and after thinning were then described as Eqs. I-11 and I-12, respectively. Eqs. I-7 and I-9 before thinning and Eqs. I-8 and I-10 after thinning were applied to generate these models.

$$R_b = (9.670 * 10^{-5} * T^2 - 5.062 * 10^{-3} * T + 0.0789) * e^{0.549*t} - 1.313 * 10^{-5} * T^2 + 2.412 * T + 0.117 \quad \text{Eq. I-11}$$

$$R_a = (9.670 * 10^{-5} * T^2 - 4.363 * 10^{-4} * T + 8.089 * 10^{-3}) * e^{0.549*t} + 0.0270 * T^2 + 5.108 * T - 30.732 \quad \text{Eq. I-12}$$

These two models were described in a three-dimensional coordinate space (Fig. I-5), with the x, y, and z axes representing growth period, temperature, and CO₂ emission rate, respectively. The total CO₂ emission rate of mushroom cultivation bottles increased exponentially as the growth stage progressed and linearly as the temperature increased.

Validation of the CO₂ Emission Models

The CO₂ emission rates estimated by the models were in good agreement with those measured (Fig. I-6). Before the thinning stage, the CO₂ emission rate estimated by the model was close to 60 $\mu\text{gCO}_2\cdot\text{s}^{-1}$, while actual values ranged from 40 to 110 $\mu\text{gCO}_2\cdot\text{s}^{-1}$.

After the thinning stage, the estimated values were in the range of 130 to 150 $\mu\text{gCO}_2\cdot\text{s}^{-1}$, but the actual values ranged between 100 and 200 $\mu\text{gCO}_2\cdot\text{s}^{-1}$.

DISCUSSION

Mycelial growth in a limited volume of growth media can be represented by logistic curves that are dependent on the carrying capacity of K^+ (Koch, 1975). In a previous study, cross-sectional images of the substrate consisting of growth media and mycelia were used to identify a stationary phase in which the ratio of mycelia to the substrate was constant. The presence of this stationary phase suggested that the mycelia of the mushrooms used in our experiments were in the latter part of the logistic growth phase. This observation is consistent with previous research showing that mycelia enter into a stationary phase after six days of incubation (Yang et al., 2011). On the other hand, the mycelial dry weights of *Flammulina velutipes* are decreased after sporophore initiation (Kitamoto and Gruen, 1976). There are two possible explanations for this observation. First, the nutrients in the medium may be reduced at the onset of the stationary phase as a result of mycelia feeding. Secondly, the nutrients may have moved to sporophores from the mycelia to facilitate sporophore growth (Chanter and Thornley, 1978). Indeed, the presence of an abundance of nutrients in the waste media of mushroom cultivation by-products has led to the use of such waste media as fodder in other applications (Kim et al., 2010). However, under the experimental conditions of the present study, the ratio of mycelium in the mixture was not decreased.

In a previous study based on image processing methods, the proportion of mycelium was determined to be greater than 60% during the entire growth period (Yang et al., 2011), while the present study identified a ratio of 30%. This difference may be due to the specific media used in the two studies: wood and corncob chips were used in the previous study, while the present study utilized sawdust. The difference in color between the media might have also affected our estimation. Therefore, it is necessary to provide a reference for estimating the proportion of mycelium when using image-based measurements. Soil respiration measurement systems can be used to measure the rate of CO₂ emission of mycelium in a given substrate (Bekku et al., 1995); however, it is difficult to measure the instantaneous respiration rate using this approach, as it relies on a blood collection syringe for gas sampling. Alternatively, respiration rates can be measured within a relatively short time by connecting the CO₂ analyzer and the chamber (Rochette et al., 1997). Likewise, since closed chamber systems are widely used for the measurement of photosynthesis to determine CO₂ consumption, an infra-red gas analyzer (IRGA) is useful to accurately measure CO₂ gas concentration (Takahashi et al., 2008).

During the thinning process, the base parts of the medium and sporophore suffer physical damage. Following these wounds, the mushroom respiration rate increases, and plant tissues age (Fonseca et al., 2002). Because the respiration of harvested mushrooms is closely related to their quality, this phenomenon has been quantified (Jacxsens et al., 2001). In this study, although there was no significant change in proportion of the mycelium (Fig. I-2), the CO₂ emission rate of the mycelium changed significantly (Table I-2). Based on this result, we inferred that the CO₂ emission rate increased due to thinning rather than

mycelium growth.

Utilizing the CO₂ emission rate models established in this study, it should now be possible to determine how CO₂ concentration increases in mushroom cultivation facilities. This should allow for development of a method for CO₂ control in mushroom cultivation, such as an optimum ventilation system. From a broader perspective, because CO₂ is one of the factors responsible for global warming, development of methods to minimize CO₂ emission will be useful for mushroom cultivation. For example, utilization of the CO₂ emitted during mushroom cultivation in plant photosynthesis has been studied (Jung et al., 2014; Kitaya et al., 1994; Tani et al., 1996).

LITERATURE CITED

- Bekku, Y., H. Koizumi, T. Nakadai, and H. Iwaki. 1995. Measurement of soil respiration using closed chamber method: an IRGA technique. *Ecological Research* 10: 369-373.
- Burton, K.S., and R. Noble. 1993. The influence of flush number, bruising and storage temperature on mushroom quality. *Postharvest Biology and Technology* 3: 39-47.
- Cannell, M.G.R., and J.H.M. Thornley. 2000. Modelling the components of plant respiration: Some guiding principles. *Annals of Botany* 85: 45-54.

- Chanter, D.O., and J.H.M. Thornley. 1978. Mycelial growth and the initiation and growth of sporophores in the mushroom crop: a mathematical model. *Journal of General Microbiology* 106: 55-65.
- Flegg, P.B., and J.F. Smith. 1982. Effect of spawn strain and available substrate on the relative yield of mushrooms in successive flushes. *Scientia Horticulturae* 17: 217-222.
- Fonseca, S.C., F.A.R. Oliveira, and J.K. Brecht. 2002. Modelling respiration rate of fresh fruits and vegetables for modified atmosphere packages: a review. *Journal of Food Engineering* 52: 99-119.
- Iwase, K. 1997. Cultivation of mycorrhizal mushrooms. *Food Reviews International* 13: 431-442.
- Jacxsens, L., F. Devlieghere, C. Van der Steen, and J. Debevere. 2001. Effect of high oxygen modified atmosphere packaging on microbial growth and sensorial qualities of fresh-cut produce. *International Journal of Food Microbiology* 71: 197-210.
- Jang, M.J., T.M. Ha, and Y.C. Ju. 2007. Comparison of respiration characteristics on the new variety of oyster mushroom according to the growth temperature. *Journal of Mushroom Science and Production* 5: 65-70.
- Jang, M.J., T.M. Ha, Y.H. Lee, and Y.C. Ju. 2009. Growth characteristics of variety of oyster mushroom (*Pleurotus ostreatus*) as affected by number of air exchanges. *Journal of Bio-Environmental Control* 18: 208-214.

- Jung, D.H., C.K. Kim, K.H. Oh, D.H. Lee, M.S. Kim, J.H. Shin, and J.E. Son. 2014. Analyses of CO₂ concentration and balance in a closed production system for king oyster mushroom and lettuce. *Korean Journal of Horticultural Science and Technology* 10: 628-635.
- Kües, U., and Y. Liu. 2000. Fruiting body production in basidiomycetes. *Applied microbiology and biotechnology* 54: 141-152.
- Kim, Y.I., J.S. Seok, and W.S. Kwak. 2010. Evaluation of microbially ensiled spent mushroom (*Pleurotus osteratus*) substrate (bed-type cultivation) as a roughage for ruminants. *Journal of animal science and technology* 52: 117-124.
- Kinugawa, K., A. Suzuki, Y. Takamatsu, M. Kato, and K. Tanaka. 1994. Effects of concentrated carbon dioxide on the fruiting of several cultivated basidiomycetes (II). *Mycoscience* 35: 345-352.
- Kitamoto, Y., and H.E. Gruen. 1976. Distribution of cellular carbohydrates during development of the mycelium and fruitbodies of *Flammulina velutipes*. *Plant Physiology* 58: 485-491.
- Kitaya, Y., A. Tani, M. Kiyota, and I. Aiga. 1994. Plant growth and gas balance in a plant and mushroom cultivation system. *Advances in Space Research* 14: 281-284.
- Koch, A.L. 1975. The kinetics of mycelial growth. *Journal of General Microbiology* 89: 209-216.
- Lee, D.J., K.P. Kim, and B.E. Lee. 2003. Studies on artificial cultivation of *Pleurotus eryngii* (De Canolle ex Freies) Quel. *The Korean Journal of Mycology* 31: 192-199.

- Rochette, P., B. Ellert, E.G. Gregorich, R.L. Desjardins, E. Pattey, R. Lessard, and B.G. Johnson. 1997. Description of a dynamic closed chamber for measuring soil respiration and its comparison with other techniques. *Canadian Journal of Soil Science* 77: 195-203.
- Ryu, J.S., M.K. Kim, S.H. Cho, Y.C. Yun, W.M. Seo, and H.S. Lee. 2005. Optimal CO₂ level for cultivation of *Pleurotus eryngii*. *Journal of Mushroom Science and Production* 3: 95-99.
- Takahashi, N., P.P. Ling, and J.M. Frantz. 2008. Considerations for accurate whole plant photosynthesis measurement. *Environmental Control in Biology* 46: 91-101.
- Tani, A., M. Kiyota, I. Aiga, K. Nitta, Y. Tako, A. Aahida, K. Otsubo, and T. Saito. 1996. Measurements of trace contaminants in closed-type plant cultivation chambers. *Advances in Space Research* 18: 181-188.
- Thronley, J.H.M. 1970. Respiration, growth and maintenance in plants. *Nature* 227: 304-305.
- Yamanaka, K. 2011. Mushroom cultivation in Japan. *WSMBMP Bulletin* 4: 1-10.
- Yang, J., J.Y. Zhao, Q. Guo, Y.S. Wang, and R.J. Wang. 2011. Data acquisition method for measuring mycelium growth of microorganism with GIS. *Computer and Computing Technologies in Agriculture IV*. Springer. pp. 374-380.
- Yang, J., J.Y. Zhao, H. Yu, L.H. Tang, and R.J. Wang. 2012. Mathematical study of the effects of temperature and humidity on the mycelium growth of *Pleurotus eryngii*. *Agro-Geoinformatics (Agro-Geoinformatics) First International Conference on 2012* pp. 1-5.

Zadražil, F. 1975. Influence of CO₂ concentration on the mycelium growth of three *pleurotus* species. European Journal of Applied Microbiology and Biotechnology 1: 327-335.

Table I-1. Parameters used in the models.

Parameter	Description
$a_1 \sim a_9$	Regression parameters
k	Relative growth rate ($\text{g} \cdot \text{g}^{-1} \cdot \text{d}^{-1}$)
M	Maintenance coefficient (s^{-1})
M_a or M_b	Maintenance coefficient (s^{-1}) after or before thinning, respectively
P	CO_2 production coefficient [$\text{gCO}_2 \cdot (\text{g dry matter})^{-1}$]
P_a or P_b	CO_2 production coefficient [$\text{gCO}_2 \cdot (\text{g dry matter})^{-1}$] after or before thinning, respectively
R	CO_2 emission rate or respiration rate ($\mu\text{gCO}_2 \cdot \text{m}^{-2} \cdot \text{s}^{-1}$)
R_a or R_b	CO_2 emission rate of mushroom per bottle ($\mu\text{gCO}_2 \cdot \text{m}^{-2} \cdot \text{s}^{-1}$) after or before thinning, respectively
R_m	CO_2 emission rate of substrate ($\mu\text{gCO}_2 \cdot \text{m}^{-2} \cdot \text{s}^{-1}$)
R_{ma} or R_{mb}	CO_2 emission rate of substrate ($\mu\text{gCO}_2 \cdot \text{m}^{-2} \cdot \text{s}^{-1}$) after or before thinning, respectively
R_s	CO_2 emission rate of sporophores ($\mu\text{gCO}_2 \cdot \text{m}^{-2} \cdot \text{s}^{-1}$)
R_{sa} or R_{sb}	CO_2 emission rate of sporophores ($\mu\text{gCO}_2 \cdot \text{m}^{-2} \cdot \text{s}^{-1}$) after or before thinning, respectively
t	Days after scratching (DAS, d)
T	Temperature ($^{\circ}\text{C}$)
W	Dry weight (g)
W_{at} or W_{bt}	Dry weight of sporophores (g) after or before thinning, respectively
W_0	Initial dry weight of sporophores (g)
W_T	Dry weight of sporophores (g) after thinning

Table I-2. CO₂ emission rate ($\mu\text{gCO}_2\cdot\text{s}^{-1}$) of the substrate according to temperature and growth period.

Growth period (DAS ^z)	Temperature (°C)					R ²
	16	18	20	22	25	
8	40.24±6.08 ^y a*	40.13±1.14a	49.61±3.05a	54.43±4.31a	59.78±4.20a	0.795
12	61.36±10.49b	68.43±4.88b	77.54±5.63b	90.28±7.08b	115.42±10.08b	0.870
15	52.39±3.54ab	76.25±7.54b	83.48±4.00b	98.69±8.74b	112.45±11.91b	0.870

*Different letters indicate a statistically significant difference (ANOVA/Duncan) ($P<0.05$)

^zDAS, days after scratching

^yMean±SD (n = 3).

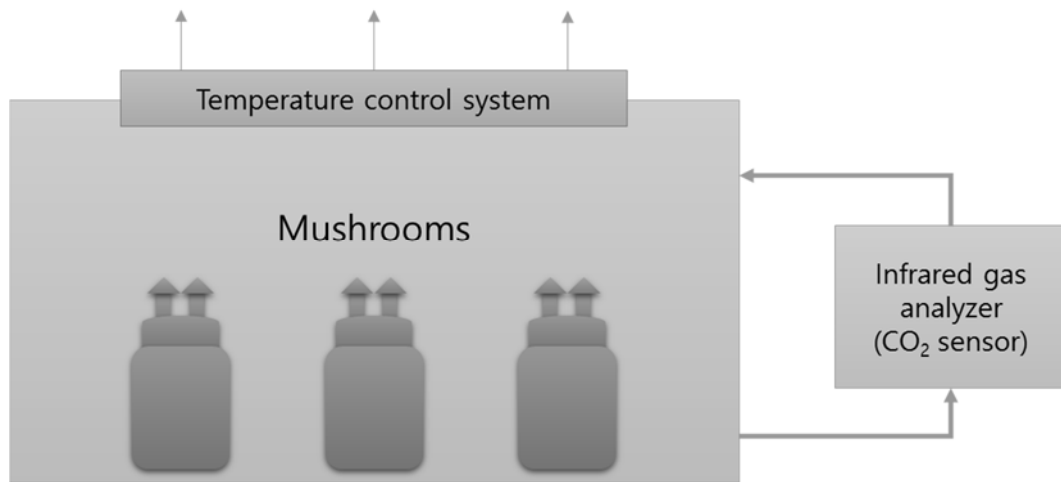


Fig. I-1. Measurement of the CO₂ emission rates of King Oyster mushrooms using a closed acrylic chamber (1.0m x 0.8m x 0.5m) in which the internal temperature was controlled within a range of 16-25°C.

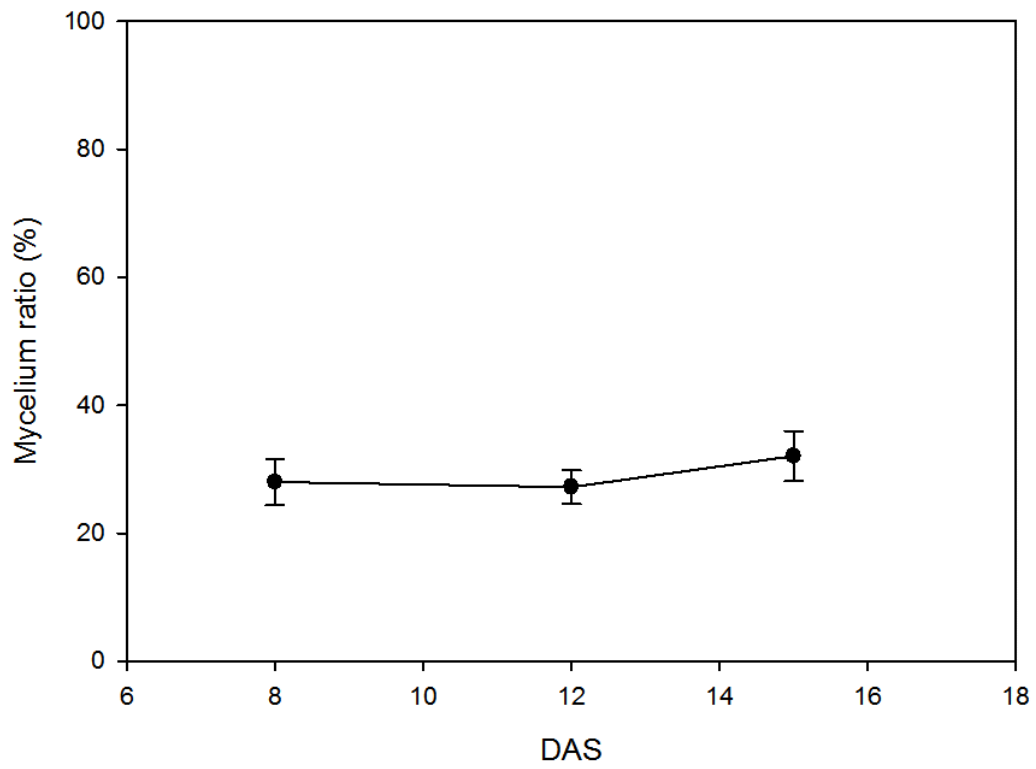


Fig. I-2. Change in the mycelium proportion of King Oyster mushrooms as a function of days after scratching (DAS). Data were collected by image processing. Vertical bars represent the mean \pm SD (n = 15).

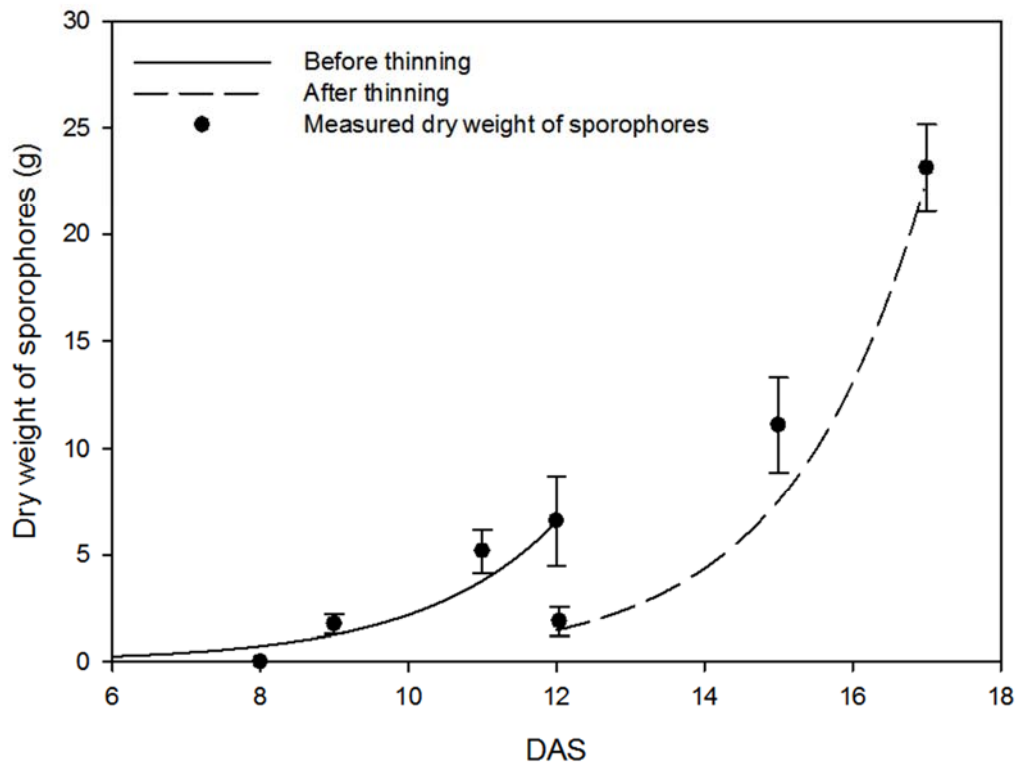


Fig. I-3. Change in the dry weight of King Oyster mushroom sporophores as a function of days after scratching (DAS). At DAS 12, all of the small sporophores were thinned, leaving only two large sporophores. Vertical bars represent the mean \pm SD (n = 15).

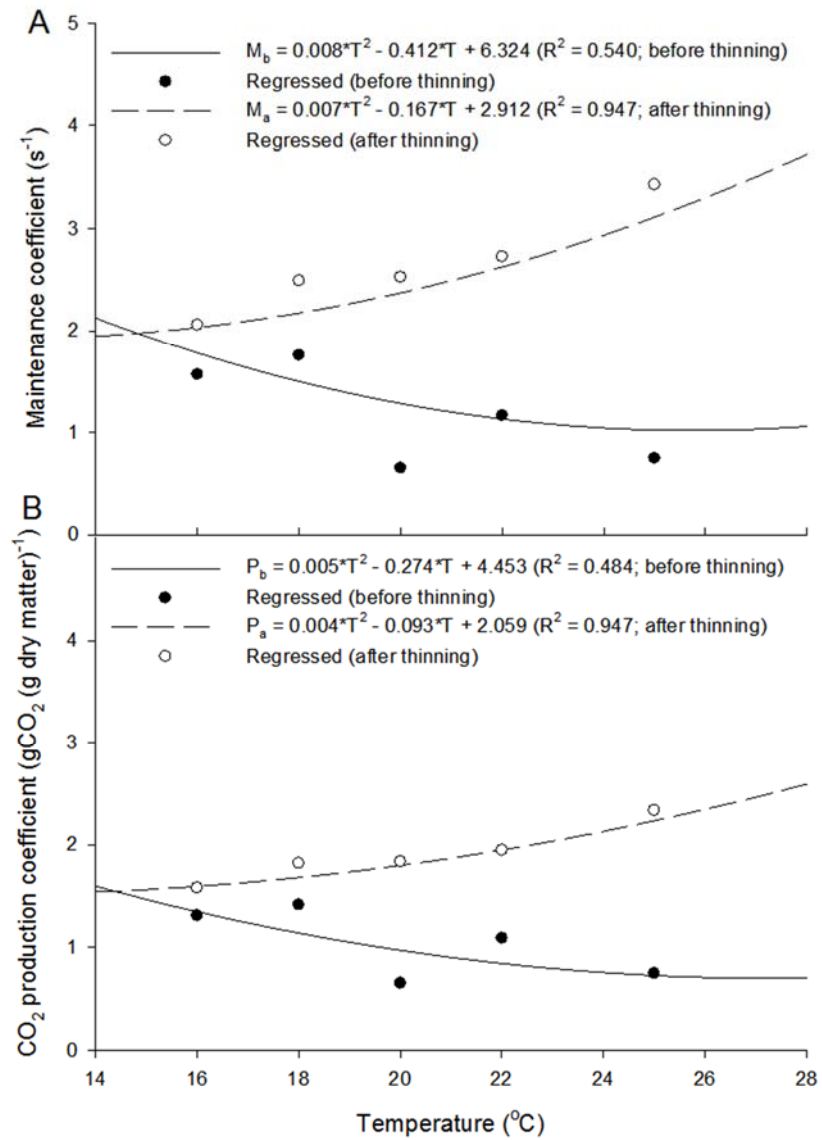


Fig. I-4. Quadratic equation regression results of the maintenance (A) and CO_2 production (B) coefficients as a function of temperature before and after thinning.

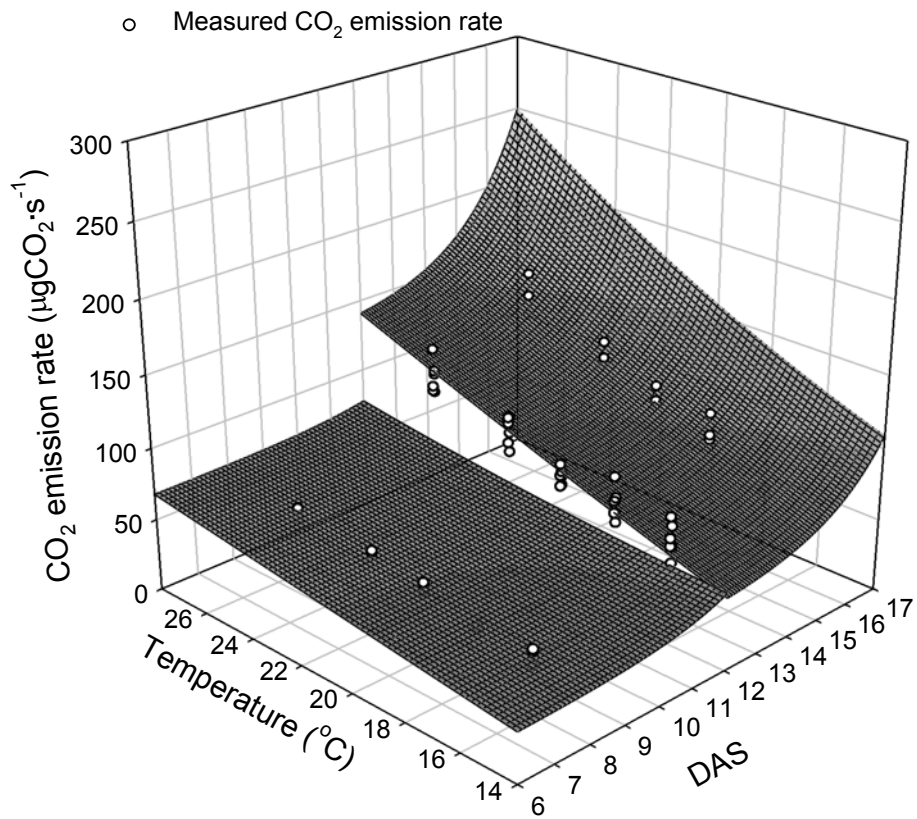


Fig. I-5. Three-dimensional diagram of the CO₂ emission rates of King Oyster mushroom cultivation bottles according to temperature and days after scratching (DAS).

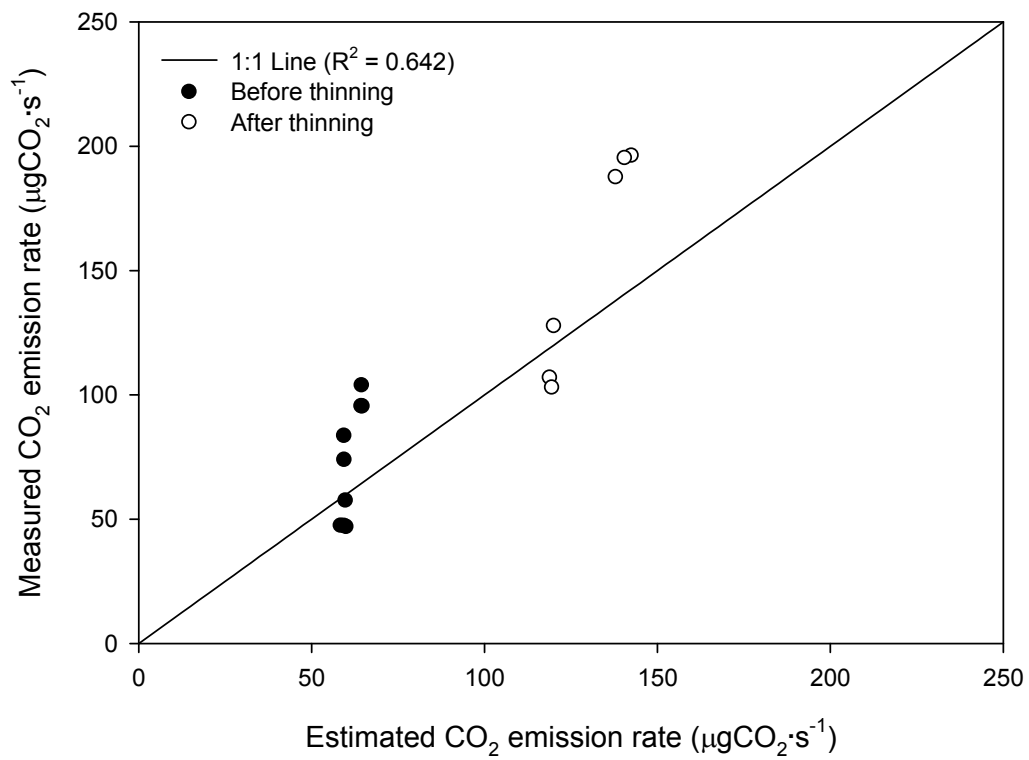


Fig. I-6. Validation of the estimated and measured CO₂ emission rates in King Oyster mushroom cultivation bottles.

CHAPTER II

Estimation of Canopy Photosynthetic Rate of Heuk Romaine Lettuce with CO₂ Concentration and Growth Stage

ABSTRACT

Since plants absorb the CO₂ in the atmosphere for photosynthesis, it is important to maintain adequate level CO₂ concentration for enhancement of crop production. To satisfy this purpose, changes in CO₂ concentration should be estimated by using photosynthetic rate models are required. The objective of this study was to estimate the canopy photosynthetic rate of romaine lettuce (*Lactuca sativa* L. 'Asia Heuk romaine') with CO₂ concentration and growth stage. Canopy photosynthetic rates of the plants were measured at 4, 7, 14, 21, and 28 days after transplanting by using closed acrylic chambers (1.0m×0.8m×0.5m), in which temperature and light intensity were maintained at 24°C and 200 μmol·m⁻²·s⁻¹ with an 8:1:1 ratio of RBW light-emitting diodes, respectively. And 2000 μmol·mol⁻¹ of initial CO₂ level were applied. By calculating the CO₂ consumption rate with time canopy photosynthetic rate of lettuce was determined. The canopy photosynthetic rate became saturated as the CO₂ concentration increased, and also showed exponential decreases with growth stage. Thornley model was suitable to express the canopy photosynthetic rate with R² = 0.985. The canopy photosynthetic rates estimated by the model were compared with those actually measured ones and showed a good agreement

with $R^2 = 0.939$. The established model can be helpful to determine the enrichment level of CO₂ concentration by growth stage and to calculate the reduced CO₂ amounts throughout cultivation period.

Additional key words: CO₂ consumption, Light-emitting diode, Light intensity, Thornley model

INTRODUCTION

As CO₂ concentration in the atmosphere becomes higher, global warming is continuously going. Since plants have abilities to fix CO₂ through photosynthesis, cultivation of plants helps to reduce the CO₂ concentration in the atmosphere. Particularly it can be better to maintain adequate level CO₂ concentration for enhancement of crop production (Leadley et al., 1999; McMurtrie and Wang, 1993). For investigating the increase in photosynthesis affected by environmental factors, it is useful to use a modeling techniques (Medina-Ruíz et al., 2011; Noe and Giersch, 2004).

Up to now, most of studies on photosynthetic model were to find out the photosynthetic reactions to environmental factors. In fact, it was difficult to make accurate models expressing photosynthesis under the complex effects of many environmental factors (Johnson et al., 2010). Thus, multivariable models have been recently used for

representing interactions of the variables in a simple multiplication form because of easiness and simplicity (Jones et al., 1991; Medina-Ruíz et al., 2011).

A model commonly used to express photosynthetic responses to light and CO₂ is a rectangular hyperbola model, showing that the photosynthetic rate increases like a saturation curve with increase of light intensity or CO₂ concentration. Thornley set a simple chemical formula for the light and dark reactions of photosynthesis (1974). By applying differential equations for each chemical formula, a rectangular hyperbola model empirically used was obtained (Kaitala et al., 1982). This model could express the change in photosynthetic rate with light intensity and CO₂ concentration, but could not express the change with growth stage. Because the light use efficiency is exponentially decreased with increase of leaf area index as plants grow (Green, 1987; Leadly et al., 1990), it is necessary to modify the model according to the growth stage.

Lettuce is a kind of leafy vegetable and easily used as a model crop for the research of plant factory. Several models were already well established for estimation of photosynthesis and growth in various cultivation systems (Caporn 1989; Shimizu et al., 2008). However, up to now, there were no attempts to apply the Thornley's multivariable model to estimate of the photosynthesis of lettuces. The objective of this study was to estimate the canopy photosynthetic rate of romaine lettuce (*Lactuca sativa* L. 'Asia Heuk romaine') with CO₂ concentration and growth stage.

MATERIALS AND METHODS

Plant and Growth Conditions

For measuring the canopy photosynthetic, Heuk romaine lettuces (*Lactuca sativa* L. ‘Asia Heuk Romaine’) were hydroponically grown in a plant factory module of Seoul National University. Yamazaki’s nutrient solutions with an electrical conductivity (EC) of $1.2 \text{ dS}\cdot\text{m}^{-1}$ were supplied to the plants. Inside temperature and light intensity were maintained at 24°C and $200 \mu\text{mol}\cdot\text{m}^{-2}\cdot\text{s}^{-1}$ with an 8:1:1 ratio of RBW light-emitting diodes (LEDs), respectively. The lettuces were transplanted 3 weeks after sowing, and grown for 4 weeks with a planting density of $25 \text{ cm}\times 25 \text{ cm}$.

Measurement of Canopy Photosynthetic Rate according to CO₂ Concentration and Growth Stage

The canopy photosynthetic rates were measured by using closed acrylic chambers ($1.0 \text{ m}\times 0.8 \text{ m}\times 0.5 \text{ m}$) at five growth stages (4, 7, 14, 21, and 28 days after transplanting; DAT), when 24, 24, 12, 8, and 8 lettuces were grown in each stage, respectively. Planting density of the plants in the chamber was set to the same during the experiment. Temperature and relative humidity were maintained at 24°C and 75%, respectively. Light intensity was $200 \mu\text{mol}\cdot\text{m}^{-2}\cdot\text{s}^{-1}$ with an 8:1:1 ratio of RBW LEDs. Initial CO₂ concentration was set at $2000 \mu\text{mol}\cdot\text{mol}^{-1}$. Changes in CO₂ concentration was measured by an infrared gas analyzer (LI-

840A, LI-COR, Lincoln, NE, USA) and controlled by a data logger (CR1000, Campbell Scientific, Logan, UT, USA). Using three chambers were used for 3 replicates. Shoot fresh and dry weights, and leaf area of the plants were measured at each growth stage.

Estimation of Intercellular CO₂ concentration

In order to express the A/C_i curve by using measured CO₂ concentration in the chambers, it is necessary to know the relationship between the atmospheric and intercellular CO₂ concentrations. Eight models express the exchange of CO₂ between atmosphere and leaves of plants (Katul et al., 2000). Among them, the Ball-Berry model has been widely used because of its simple form as follows:

$$\frac{C_i}{C_a} = 1 - \frac{1}{m} * \frac{1}{RH} \quad \text{Eq. II-1}$$

where, C_i and C_a are the intercellular and atmospheric CO₂ concentrations ($\mu\text{mol}\cdot\text{mol}^{-1}$), respectively. RH is the relative humidity and m is an empirical parameter. In fact, m ranges from 3 to 10 for various plant species, but has not been reported for lettuce (Leuning, 1995). The symbols used in the models were summarized in Table II-1. To estimate the m value of lettuce, C_i , C_a and RH values were measured by an using leaf photosynthesis system (LI-6400, LI-COR, Lincoln, NE, USA) and regressed with Eq. II-1.

Establishment of Canopy Photosynthetic Rate Model according to CO₂ Concentration and Growth Stage

Using atmospheric CO₂ concentration measured over time in the chambers, its moving average of 12 minutes was calculated. The CO₂ concentrations measured in each growth stage were converted to the intercellular CO₂ concentration by using Eq. II-1

Photosynthetic rate with CO₂ concentration was obtained by using Eq. II-2 (Thornley, 1974).

$$P = \frac{a*b*PPFD*C_i}{a*PPFD+b*C_i} + c \quad \text{Eq. II-2}$$

where, P means the photosynthetic rate ($\mu\text{molCO}_2\cdot\text{m}^{-2}\cdot\text{s}^{-1}$) and $PPFD$ is the photosynthetic photon flux density ($\mu\text{mol}\cdot\text{m}^{-2}\cdot\text{s}^{-1}$). a , b , and c are the photochemical efficiency ($\mu\text{molCO}_2\cdot\mu\text{mol}^{-1}$), carboxylation conductance (s^{-1}), and dark respiration ($\mu\text{molCO}_2\cdot\text{m}^{-2}\cdot\text{s}^{-1}$), respectively. Because the light use efficiency is exponentially reduced, a decrease in photosynthetic rate with growth stage could be expressed as follows:

$$P = p * e^{-q*DAT} \quad \text{Eq. II-3}$$

where, DAT is the days after transplanting, and p and q are regression parameters.

A simple multiplication model (Eq. II-4) was developed by multiplying Eqs. II-2 and II-3 as follows:

$$P = \left(\frac{a*b*PPFD*C_i}{a*PPFD+b*C_i} + c \right) * (p * e^{-q*DAT}) \quad \text{Eq. II-4}$$

By inserting Eq. II-1 to Eq. II-4 a photosynthetic rate model (Eq. II-5) was obtained as follows:

$$P = \frac{p_1*p_2*e^{-(q_1+q_2)*DAT}*PPFD*C_i}{p_1*e^{-q_1*DAT}*PPFD+p_2*e^{-q_2*DAT}*C_i} + p_3 * e^{-q_3*DAT} \quad \text{Eq. II-5}$$

All the regression parameters in the simple multiplication model and Thornley model were analyzed using a statistical program SPSS (IBM, New York, NY, USA).

Validation of the Simple Multiplication Model and Thornley Model

The simple multiplication model and Thornley model were validated with linear regression analysis by comparing the measured and estimated canopy photosynthetic rates. For validation, the plants grown in the same period were used when the models established.

RESULTS

Shoot Fresh and Dry Weights, and Leaf Area according to Growth Stage

Shoot fresh and dry weight, and leaf area increased exponentially according to growth stage (Fig. II-1). The shoot fresh and dry weights, and leaf area were 154.58 ± 56.79 g, 5.40 ± 1.95 g, and 2595.57 ± 770.65 cm² at DAT 28, respectively. Especially, the leaf area (LA) was regressed as following exponential model:

$$LA = 64.76 * e^{0.132*DAT} \quad \text{Eq. II-6}$$

The value of R² in the model was estimated to be 0.849.

Intercellular CO₂ Concentration

Intercellular CO₂ concentration increased linearly according to atmospheric CO₂ concentration (Fig. II-2). As the atmospheric CO₂ concentration increased from 100 to 1000 $\mu\text{mol}\cdot\text{mol}^{-1}$, the intercellular CO₂ concentration increased from 80 to 800 $\mu\text{mol}\cdot\text{mol}^{-1}$, respectively. The m value in Eq. II-1 was estimated to be 5.041 at a RH of 75%. The value of R^2 in the Ball-Berry model (Eq. II-1) was estimated to be 0.968.

Canopy Photosynthetic Rate Models according to Intercellular CO₂ Concentration and Growth Stage

Canopy photosynthetic rate of the plants according to intercellular CO₂ concentration increased showing a saturation curve (Fig. II-3). The CO₂ compensation points were estimated to be 70 $\mu\text{mol}\cdot\text{mol}^{-1}$ in all the growth stage. The maximum canopy photosynthetic rates were 26, 22, 16, 8, and 5 $\mu\text{molCO}_2\cdot\text{m}^{-2}\cdot\text{s}^{-1}$ at DAT 4, 7, 14, 21, and 28, respectively. The maximum canopy photosynthetic rates decreased exponentially as growth stage progresses. The canopy photosynthetic rate was saturated over an intercellular CO₂ concentration of 1200 $\mu\text{mol}\cdot\text{mol}^{-1}$ at DAT 4 and 7, 1000 $\mu\text{mol}\cdot\text{mol}^{-1}$ at DAT 14, and 800 $\mu\text{mol}\cdot\text{mol}^{-1}$ at DAT 21 and 28.

A regression analysis result for the simple multiplication model was shown in Fig. II-5 A. The canopy photosynthetic rate decreased exponentially as growth stage progresses. And the canopy photosynthetic rate increased as a saturation curve as intercellular CO₂ concentration increases. By regression analysis, the parameters of a , b , c , p and q in

Eq. II-4 were estimated to be 0.688, 0.904, -42.694, 0.406 and 0.055, respectively. The simple multiplication model was expressed as follows:

$$P = \left(\frac{124.3904 * C_i}{137.6 + 0.904 * C_i} - 42.694 \right) * 0.406 * e^{-0.055 * DAT} \quad \text{Eq. II-7}$$

The value of R^2 in the model was estimated to be 0.985.

The photochemical efficiency, carboxylation conductance, and dark respiration in Eq. II-2 were regressed with high R^2 values according to growth stage (Table II-2). The photochemical efficiency and carboxylation conductance decreased exponentially, while the dark respiration increased exponentially (Fig. II-4). As results, Thornley model could be expressed as follows (Fig. II-5 B).

$$P = \frac{21.812 * e^{-0.107 * DAT} * C_i}{57.4 * e^{-0.057 * DAT} + 0.380 * e^{-0.050 * DAT} * C_i} - 18.608 * e^{-0.056 * DAT} \quad \text{Eq. II-8}$$

The value of R^2 in the model was estimated to be 0.985.

Validation of the Simple Multiplication Model and Thornley Model

The canopy photosynthetic rates estimated by the simple multiplication model and Thornley model showed good agreements with measured ones (Fig. II-6). The values of R^2 in the two models were estimated to be the same value of 0.939. However in early stages of DAT 4 and 7, the measured canopy photosynthetic rates were slightly lower than the estimated ones.

DISCUSSION

It is preferred to use CO₂ flux for expressing leaf photosynthesis. However for several plants in the chamber, canopy photosynthesis can be expressed as CO₂ absorption per plant. Thus, the leaf area model as Eq. II-6 can be used when the photosynthetic rate of one plant is required in the canopy.

Various types of chamber are used for the measurement of photosynthesis (Mitchell, 1992), and the closed types are mainly used for the measurement of canopy photosynthesis. The closed systems have an advantage in its simple equipment, but a disadvantage of difficulty in measuring the steady state photosynthesis (Bugbee, 1992). Thus, the Thornley's dynamic photosynthesis model is more appropriate to use measured canopy photosynthetic rates.

In measuring the photosynthetic rates of willow plants at a light intensity of 220 $\mu\text{mol}\cdot\text{m}^{-2}$, the photochemical efficiency and carboxylation conductance were estimated to be 0.00028 $\mu\text{mol}^{-1}\cdot\text{m}^2$ and 0.001053 $(\text{kg CO}_2 \text{ m}^{-3})\cdot\text{s}^{-1}$, respectively (Kaitala et al., 1982). And the photochemical efficiency of *Atriplex hastata*, was estimated to be 0.177 $\mu\text{molCO}_2\cdot\mu\text{mol}^{-1}$ (Marshall and Biscoe, 1980). However, these studies did not track the changes in photochemical efficiency and carboxylation conductance with growth stage. In this study, the photochemical efficiency and carboxylation conductance of the lettuce tended to exponentially decrease as growth stage progresses.

A simple multiplication model could be easily applied because of its simplicity in the form. However, in order to express the changes in photochemical efficiency and

carboxylation conductance according to growth period, Thornley model can be better because it reflects the physiological reactions of the plants. The R^2 values of the simple multiplication model and Thornley model were 0.985 when regressed and 0.939 when validated. Although the both R^2 values were reliable, it is better to use Thornley model because it reflects the physiological reactions.

From many studies on various plant species, it was known that CO₂ enrichment is effective to increase the plant biomass (Leadley et al., 1999). Quantification of the CO₂ consumption through photosynthesis will help to establish the efficient CO₂ enrichment strategies in plant production. It can also be coupled with microclimate models reflecting environmental conditions in greenhouse or plant factory for adequate management of crop cultivation.

LITERATURE CITED

- Bugbee, B. 1992. Steady-state canopy gas exchange: system design and operation. HortScience 27: 770-776.
- Caporn, S.J.M. 1989. The effects of oxides of nitrogen and carbon dioxide enrichment on photosynthesis and growth of lettuce (*Lactuca sativa* L.). New Phytology 111: 473-481.
- Green, C.F. 1987. Nitrogen nutrition and wheat growth in relation to absorbed solar radiation. Agricultural and Forest Meteorology 41: 207-248.
- Johnson, I.R., J.H.M. Thornley, J.M. Frantz, and B. Bugbee. 2010. A model of canopy

- photosynthesis incorporating protein distribution through the canopy and its acclimation to light, temperature and CO₂. *Annals of Botany* 106: 735-749.
- Jones, J.W., E. Dayan, L.H. Allen, H. Van Keulen, and H. Challa. 1991. A dynamic tomato growth and yield model (TOMGRO). *Transactions of the ASABE* 34: 663-672.
- Kaitala, V., P. Hari, E. Vapaavuori, and R. Salminen. 1982. A dynamic model for photosynthesis. *Annals of Botany* 50: 385-396.
- Katul, G.G., D.S. Ellsworth, and C.T. Lai. 2000. Modelling assimilation and intercellular CO₂ from measured conductance: a synthesis of approaches. *Plant, Cell and Environment* 23: 1313-1328.
- Leadley, P.W., J.F. Reynolds, R. Flagler, and A.S. Heagle. 1990. Radiation utilization efficiency and the growth of soybeans exposed to ozone: a comparative analysis. *Agricultural and Forest Meteorology* 51: 293-308.
- Leadley, P.W., P.A. Niklaus, and R. Stocker. 1999. A field study of the effects of elevated CO₂ on plant biomass and community structure in a calcareous grassland. *Oecologia* 118: 39-49.
- Leuning, R. 1995. A critical appraisal of a combined stomatal-photosynthesis model for C₃ plants. *Plant Cell and Environment* 18: 339-355.
- Marshall, B., and P.V. Biscoe. 1980. A model for C₃ leaves describing the dependence of net photosynthesis on irradiance. *Journal of Experimental Botany* 31: 29-39.
- McMurtrie, R.E., and Y.P. Wang. 1993. Mathematical models of the photosynthetic response of tree stands to rising CO₂ concentrations and temperatures. *Plant, Cell and Environment* 16: 1-13.

- Medina-Ruíz, C.A., I.A. Mercado-Luna, G.M. Soto- Zarazúa, I. Torres-Pacheco, and E. Rico-García. 2011. Mathematical modeling on tomato plants: A review. *African Journal of Agricultural Research* 6: 6745-6749.
- Mitchell, C.A. 1992. Measurement of photosynthetic gas exchange in controlled environments. *HortScience* 27: 764-767.
- Noe, S.M., and C. Giersch. 2004. A simple dynamic model of photosynthesis in oak leaves: coupling leaf conductance and photosynthetic carbon fixation by a variable intercellular CO₂ pool. *Functional Plant Biology* 31: 1195-1204.
- Shimizu, H., M. Kushida, and W. Fujinuma. 2008. A growth model for leaf lettuce under greenhouse environments. *Environmental Control in Biology* 46: 211-219.
- Thornley, J.H.M. 1974. Light fluctuations and photosynthesis. *Annals of Botany* 38: 363-373.

Table II-1. Parameters used in the models.

Parameter	Description
C_i	Intercellular CO ₂ concentration ($\mu\text{mol}\cdot\text{mol}^{-1}$)
C_a	Atmospheric CO ₂ concentration ($\mu\text{mol}\cdot\text{mol}^{-1}$)
RH	Relative humidity
m	An empirical parameter
P	Canopy photosynthetic rate ($\mu\text{molCO}_2\cdot\text{m}^{-2}\cdot\text{s}^{-1}$)
$PPFD$	Light intensity ($\mu\text{mol}\cdot\text{m}^{-2}\cdot\text{s}^{-1}$)
a	Photochemical efficiency ($\mu\text{molCO}_2\cdot\mu\text{mol}^{-1}$)
b	Carboxylation conductance (s^{-1})
c	Dark respiration ($\mu\text{molCO}_2\cdot\text{m}^{-2}\cdot\text{s}^{-1}$)
DAT	Days after transplanting (d)
p and q	Regression parameters
LA	Leaf area (cm^2)

Table II-2. Regression results of photochemical efficiency, carboxylation conductance, dark respiration, and R² values.

DAT	Photochemical efficiency ($\mu\text{molCO}_2\cdot\mu\text{mol}^{-1}$)	Carboxylation conductance (s^{-1})	Dark respiration ($\mu\text{molCO}_2\cdot\text{m}^{-2}\cdot\text{s}^{-1}$)	R ²
4	0.235	0.333	-15.967	0.970
7	0.182	0.258	-12.004	0.995
14	0.146	0.225	-9.564	0.995
21	0.085	0.134	-5.825	0.992
28	0.054	0.070	-3.374	0.997

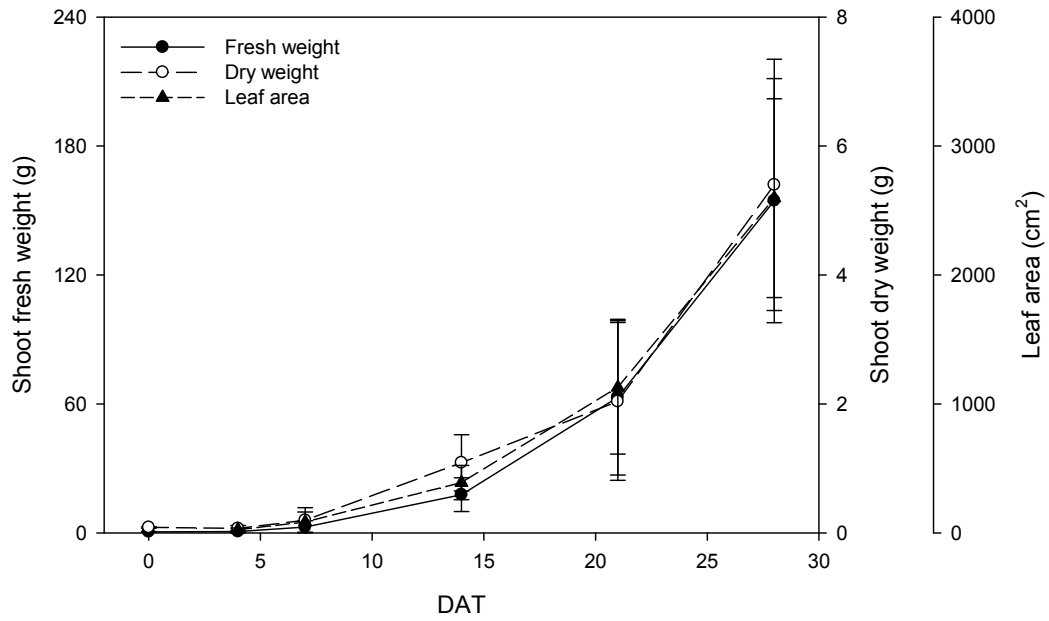


Fig. II-1. Measured shoot fresh (solid circle and solid line) and dry (void circle and medium dash) weights, and leaf area (solid triangle and short dash) of the lettuce with growth stage. Vertical bars represent the mean \pm SD (n = 15).

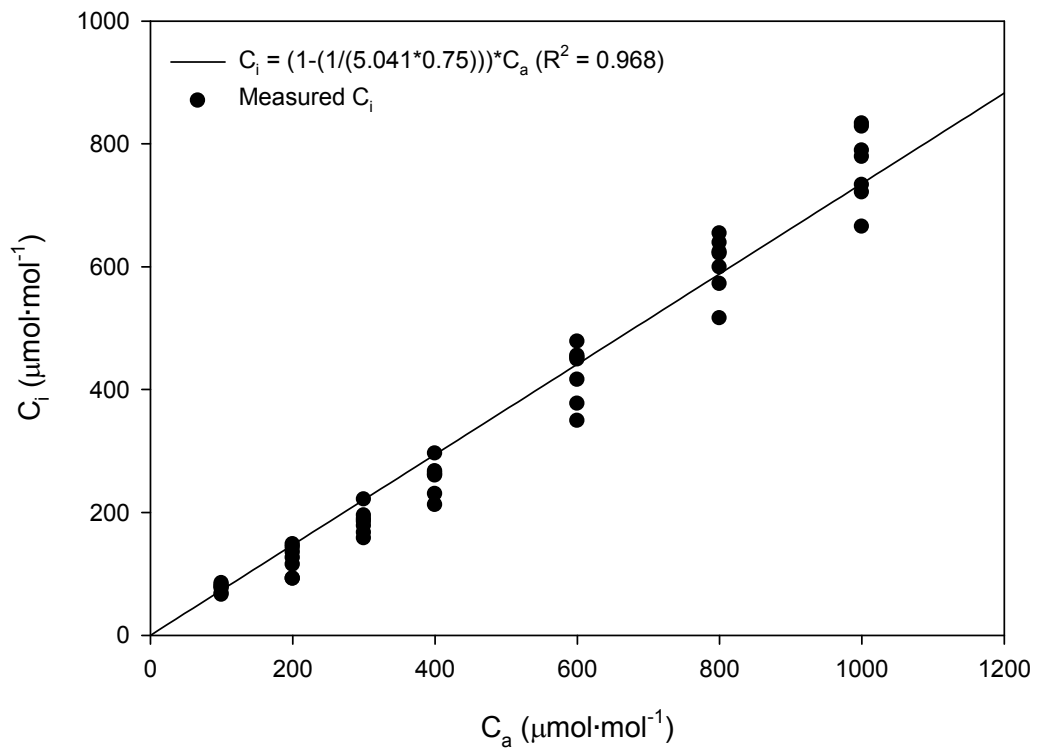


Fig. II-2. Relationship between atmospheric (C_a) and intercellular (C_i) CO_2 concentrations in the lettuce leaves. The m value in the Ball-Berry model was used for C_i .

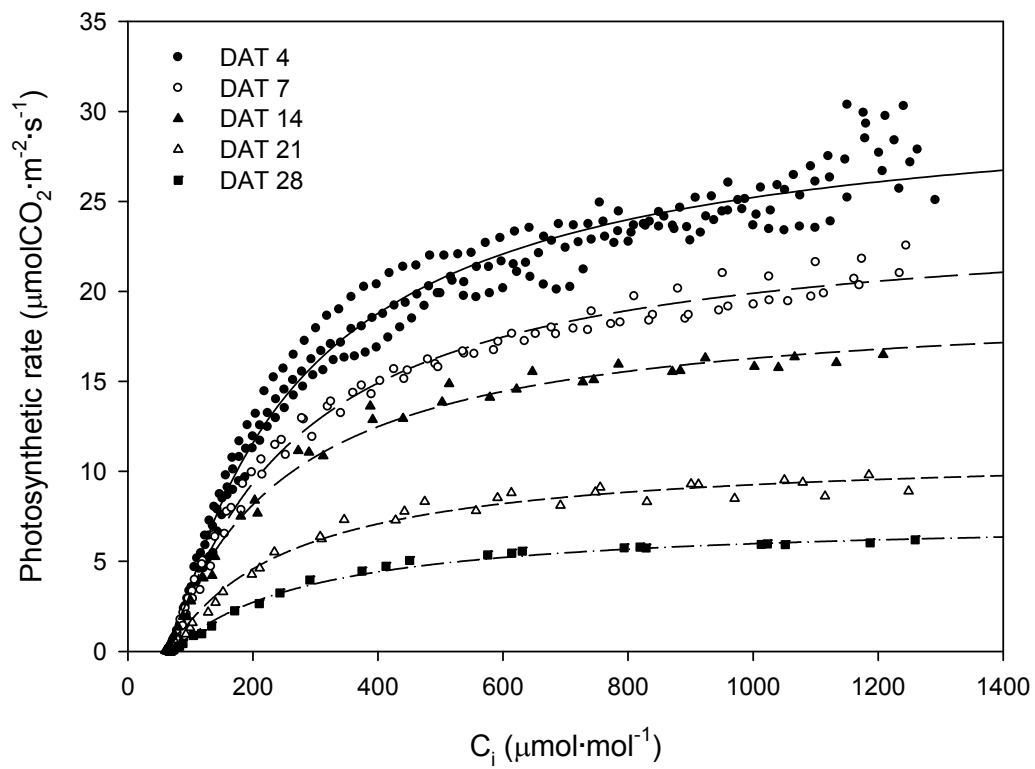


Fig. II-3. Regressed A/C_i curves at difference growth stages of DAT 4 (solid), 7 (long dash), 14 (medium dash), 21 (short dash) and 28 (dash-dot). The symbols mean the measured photosynthetic rates of the lettuce at DAT 4 (solid circle), 7 (void circle), 14 (solid triangle), 21 (void triangle) and 28 (solid square).

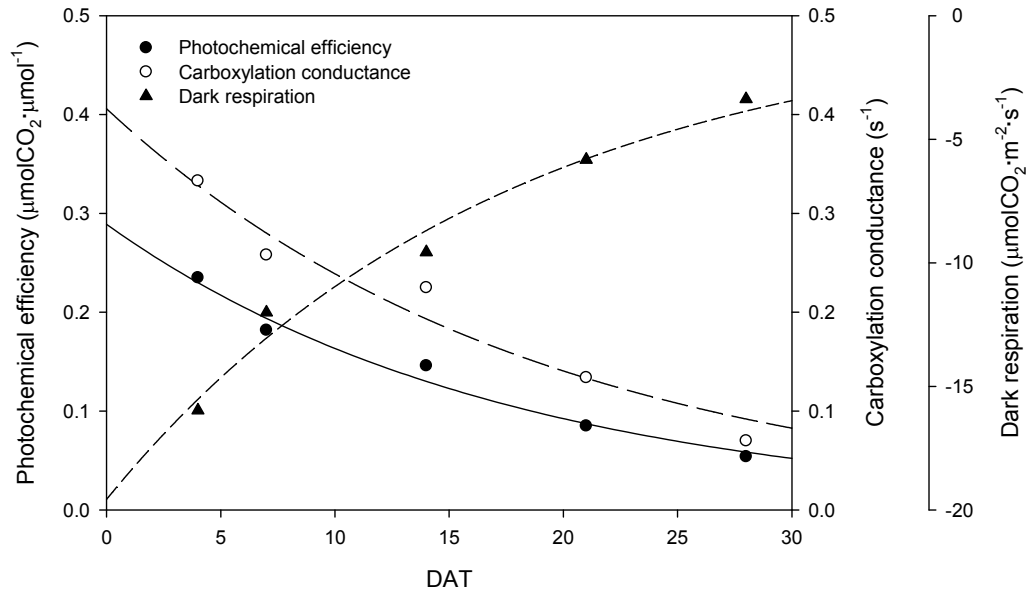


Fig. II-4. Regressed results of photochemical efficiency (solid circle), carboxylation conductance (void circle), and dark respiration (solid triangle).

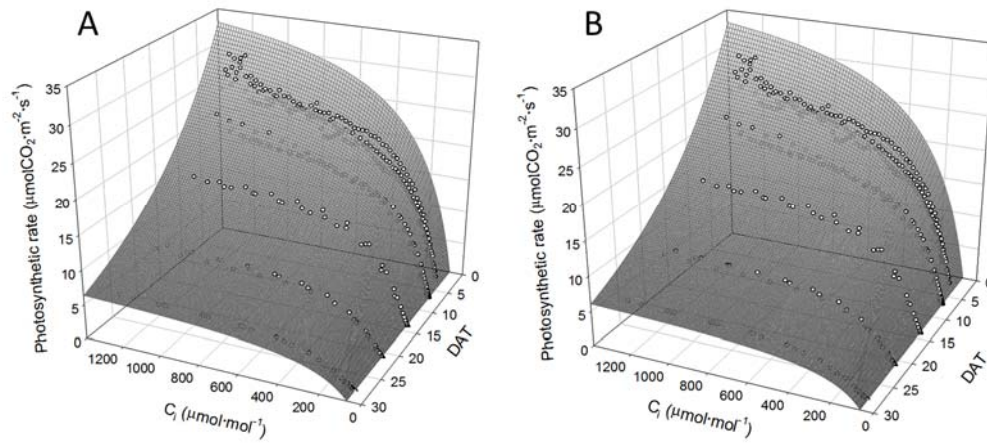


Fig. II-5. Regressed results of the simple multiplication model (A) and Thornley model (B) of canopy photosynthetic rates according to intercellular CO_2 concentration and growth stage. White circles mean the measured canopy photosynthetic rates of the lettuce.

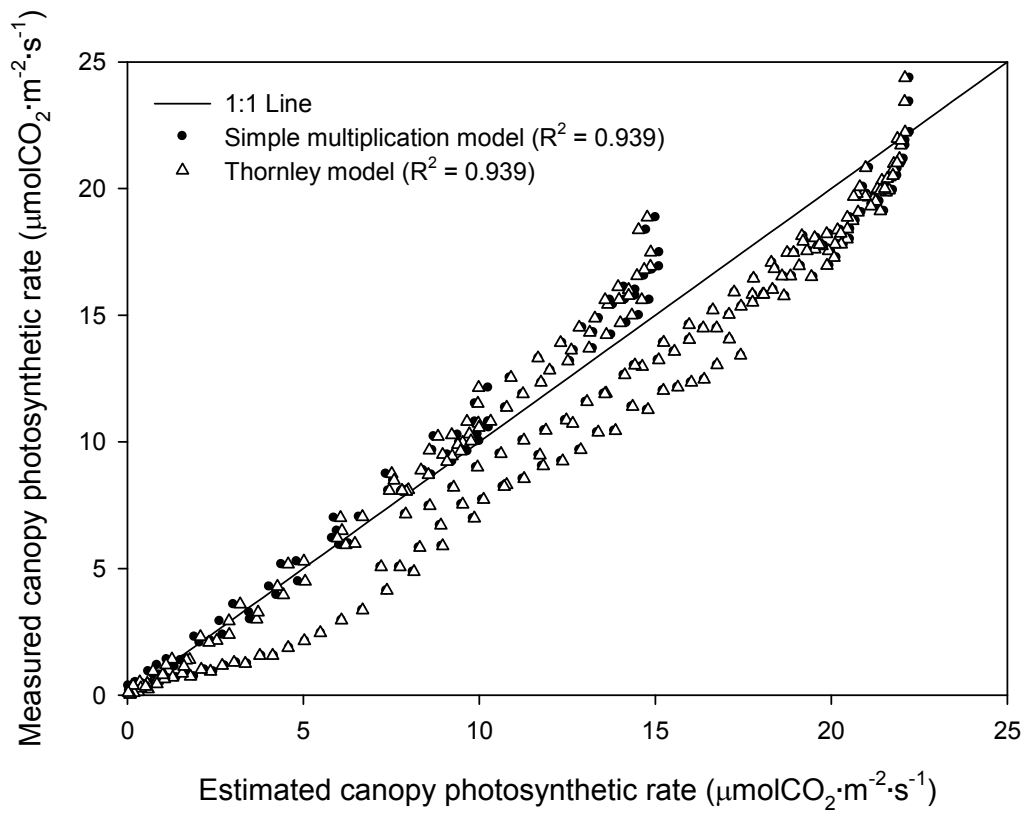


Fig. II-6. Validation of canopy photosynthetic rates of the simple multiplication model and Thornley model.

CHAPTER III

Continuous Cultivation Strategies with CO₂ Control for a Closed Production of King Oyster Mushrooms and Romaine Lettuces

ABSTRACT

Since a large amount of CO₂ gas emitted from mushrooms is useful for plant photosynthesis and plant growth, more systematic approach for mixed cultivation of mushrooms and plants is required. The objective of this study was to establish an appropriate cultivation strategy for CO₂ balance in a closed production of mushroom and lettuce by using a CO₂ emission rate model of mushroom and a photosynthetic rate model of lettuce. A closed plant production system consisting of three lettuce chambers, one mushroom chamber, and one gas-mixing chamber were established. Simulations were conducted at two cultivation conditions in the closed plant production system by using MATLAB: One was to put all the lettuces and mushrooms into the chambers and the other was to put them step by step. The lettuce and mushroom chambers were stably maintained over 1000 $\mu\text{mol}\cdot\text{mol}^{-1}$ and under 2000 $\mu\text{mol}\cdot\text{mol}^{-1}$, respectively, in the continuous cultivation. During the 5 days, shoot fresh weights increased about 20 to 30% at all growth stages. Compared to the single cultivation of mushrooms, the mixed cultivation of mushrooms and lettuces could reduce the CO₂ emissions into the atmosphere by 80.6%. It is concluded that the simultaneous cultivation strategy of mushroom and lettuce will reduce

the greenhouse gas emissions and applied to the closed plant production such as space agriculture.

Additional key words: Canopy photosynthesis, CO₂ balance, CO₂ emission, Mushroom respiration, Simulation

INTRODUCTION

Since mushrooms are aerobic fungi, a large amount of CO₂ gas in mushroom cultivation are emitted by respiration into the atmosphere as greenhouse gas (Thavivongse and Buppachat, 2013). In addition, CO₂ gases of high concentration suppress the growth of mushrooms (Jang et al., 2009), but is useful for enhancement of plant biomass production (Leadley et al., 1999).

In the research of Controlled Ecological Life Support System (CELSS), plants were designed to absorb the CO₂ generated by human respiration (Daunicht, 1997). However, these studies differ from the plant production systems conducting an efficient crop growth through an active usage of CO₂ gas (Son et al., 1999). There was an attempt to supply the CO₂ generated by mushrooms during cultivation to lettuces (Kitaya et al., 1994). However the amount of mushrooms was not quantified because bag cultures were used. For an accurate analysis of CO₂ behaviors, the simultaneous cultivation of lettuces and mushrooms

for a long cultivation periods are required. Jung et al. (2014) just showed the changes in CO₂ concentration with growth stage and the ratio of lettuces and mushrooms. For sustainable cultivation, the amounts of CO₂ emitted and consumed by lettuces and mushrooms, respectively, should be equal over time.

These problems can be solved by continuous (conveyer) cultivations where plants at several growth stage groups are simultaneously plated to the cultivation systems (Gitelson et al., 2003). The continuous cultivation method has an advantage of smaller fluctuations in CO₂ concentration than the method to input all the plants at a time. However, these cultivation systems are actually difficult to manage because it includes various environmental variables as well as it is difficult to track the interaction of each variable (Hendrickx et al., 2006). For adequate investigation of such complicated systems, simulation methods are essentially required (Volk and Rummel, 1987). In this study, a simultaneous cultivation system of lettuce and mushroom was analyzed by simulation methods.

The objectives of this study were to find a cultivation method to archive equilibrium concentration of CO₂ by circulating a gas between the cultivation chambers and confirm the difference between the CO₂ concentration which measured actually and predicted by the simulation method.

MATERIALS AND METHODS

Cultivation Conditions

Heuk romaine lettuces (*Lactuca sativa* L. ‘Asia Heuk Romaine’) at DAT 0, 5, 10, 15, and 20 were used for the experiment. Yamazaki’s nutrient solutions with an electrical conductivity (EC) of $1.2 \text{ dS}\cdot\text{m}^{-1}$ were supplied to the plants. Inside temperature and light intensity were maintained at 24°C and $200 \mu\text{mol}\cdot\text{m}^{-2}\cdot\text{s}^{-1}$ with an 8:1:1 ratio of RBW light-emitting diodes (LEDs), respectively. Three lettuces were used at each growth stage in each chamber. Photoperiods in the lettuce chambers were shown in Table III-2. King Oyster mushrooms (*Pleurotus eryngii* (DC.) Quél) at DAS 3, 7, 11, and 15 were used for the experiment. Three mushroom bottles at each growth stage were placed in the mushroom chamber.

Cultivation Systems

For simulation and verification of simultaneous cultivations of lettuces and mushrooms, a system consisted of three lettuce chambers, one mushroom chamber, and one mixing chamber was constructed (Fig. III-1). The size of the lettuce and mushroom chambers was 400 L ($1.0 \text{ m} \times 0.8 \text{ m} \times 0.5 \text{ m}$) and that of the mixing chamber was 125 L ($0.5 \text{ m} \times 0.5 \text{ m} \times 0.5 \text{ m}$). Each chamber was made by acryl plates and completely sealed during experimental periods. Temperatures in the lettuce and mushroom chambers were maintained at 24°C and 18°C , respectively. Air in the chambers was circulated at a flow

rate of $62 \text{ L}\cdot\text{min}^{-1}$ between chambers by a diaphragm pump (Boxer 7004, Uno International Ltd., London, UK). CO_2 generated in the mushroom chamber did not go directly to the lettuce chambers, and it moved through the mixing chambers. The mixing chamber was designed to allow gas exchanges with the external air, because it prepares for the case of CO_2 concentration in the total system excessing or depleting.

CO₂ Measurement

CO_2 concentration in each chamber was measured every two minutes using an infrared CO_2 sensor (LI-820, LI-COR, Lincoln, NE, USA) controlled by a data logger (CR1000, Campbell Scientific, Logan, UT, USA). The pumps between lettuce and mixing chamber, between the mushroom and mixing chamber, and between the mixing chamber and the external air were operated when the CO_2 concentrations in each lettuce chamber became below $1000 \mu\text{mol}\cdot\text{mol}^{-1}$, when in the mushroom chamber over $2000 \mu\text{mol}\cdot\text{mol}^{-1}$, and in the mixing chamber over $2000 \mu\text{mol}\cdot\text{mol}^{-1}$. AC/DC controllers (SDM-CD16AC, Campbell Scientific Inc., Logan, UT, USA) were used to control the diaphragm pumps.

Simulation Models

Following governing equations were used to express the CO_2 behavior in the cultivation systems:

$$V * \frac{dC_{L1}}{dt} = (C_X - C_{L1}) * Q_{L1} - LN1 * P1 \quad \text{Eq. III-1}$$

$$V * \frac{dC_{L2}}{dt} = (C_X - C_{L2}) * Q_{L2} - LN2 * P2 \quad \text{Eq. III-2}$$

$$V * \frac{dC_{L3}}{dt} = (C_X - C_{L3}) * Q_{L2} - LN3 * P3 \quad \text{Eq. III-3}$$

$$V * \frac{dC_M}{dt} = (C_X - C_M) * Q_M + MN * R \quad \text{Eq. III-4}$$

$$V * \frac{dC_X}{dt} = (C_{L1} - C_X) * Q_{L1} + (C_{L2} - C_X) * Q_{L2} + (C_{L3} - C_X) * Q_{L3} \\ + (C_M - C_X) * Q_M + (C_O - C_X) * Q_X \quad \text{Eq. III-5}$$

The symbols used in the models are summarized in Table III-1. Initial CO₂ concentrations in the lettuce, mushroom, and mixing chambers was 1000, 500, and 1000 μmol·mol⁻¹, respectively. Ambient CO₂ concentration was assumed as 500 μmol·mol⁻¹.

Simulation Conditions

Accumulated photosynthetic rates in the lettuce chambers (*P1 ~ P3*) were calculated using Eqs. II-6 and II-8. And accumulated CO₂ emission rates in the mushroom chamber (*R*) was calculated using Eqs. I-11 and I-12. Three lettuces were added to the lettuce chamber every 5 days, and three mushroom bottles were added to the mushroom chamber every 4 days (Fig. III-2). The pumps among the lettuce chambers and mixing chamber (*Q_{L1~L3}*) were operated when the CO₂ concentration in each lettuce chamber became below 1000 μmol·mol⁻¹, while the pumps between the mushroom chamber and mixing chamber (*Q_M*) operated when the CO₂ concentration in the mushroom chamber became over 2000 μmol·mol⁻¹. The pumps between the mixing chamber and the external air (*Q_X*) were operated when the CO₂ concentration in the mixing chamber became over 2000 μmol·mol⁻¹. The photoperiod in the lettuce chambers were shown in Table III-2. Simulations were conducted to estimate the CO₂ concentration in each chamber for 3 days

by using MATLAB (Mathworks, Natick, MA, USA). CO₂ emissions from the mixing chamber to the external air were calculated.

Experimental Conditions for Verification

Verification experiments were carried out for 5 days. Shoot fresh weight and leaf area of the lettuces at each growth stage were measured before and after the experiment. Also, in order to compare the growth of the lettuce used in the experiment, lettuces were grown in the chambers that the other environmental conditions were the same except for the CO₂ concentration. And the accumulated CO₂ amounts from the mixing chamber to the external air were calculated. All the experimental conditions were the same as described in the simulation.

RESULTS AND DISCUSSION

CO₂ Concentrations in Lettuce and Mushroom Chambers

The measured and estimated CO₂ concentrations in the lettuce and mushroom chambers were compared (Fig. III-3). The CO₂ concentration in the lettuce chambers were controlled by the set point of 1000 $\mu\text{mol}\cdot\text{mol}^{-1}$ or higher (Fig. III-3 A ~ C). However, the CO₂ concentration of the lettuce chambers falls below the set point (Fig. III-3 D). This phenomenon is considered to occur when the pumps are operating at a lower CO₂

concentration of the mixing chambers (Fig. III-3 E). It can be confirmed from the period of the CO₂ concentration in the mixing chamber becomes lower to the period of the CO₂ concentration in the lettuce chambers becomes lower is consistent. In addition, the respiration rates of the lettuces in the verification experiment are lower than the respiration rate of the lettuces in the simulation.

From the results, it is confirmed that the gas exchange also took place due to the malfunction of pumps during dark period in the lettuce chambers, while the CO₂ concentration in the mushroom chamber was well controlled below the set point of 2000 $\mu\text{mol}\cdot\text{mol}^{-1}$. When the CO₂ concentration in the mushroom cultivation facilities is below 2400 $\mu\text{mol}\cdot\text{mol}^{-1}$, marketable values of King Oyster mushrooms appeared much higher (Ryu et al., 2005). Therefore, when applying the simultaneous cultivation method, the CO₂ concentration should be maintained at an appropriate level.

The shoot fresh weight and leaf area of the lettuces grown for significantly increased 5 days except for leaf area at DAT 25 (Table III-3). Particularly, the shoot fresh weight increased about 20 to 30% at all growth stages.

Accumulated CO₂ Emission into the Atmosphere

The accumulated CO₂ emission from the mixing chamber into the atmosphere was estimated to be 35 g for 3 days, while actual value was 48 g (Fig. III-4). Because the CO₂ was emitted only when the pumps are operating, the accumulated CO₂ emission with time appeared as a step-like. If the only mushrooms are cultivated, the simulation results might be 180 g of CO₂ emission during the 3 days. Therefore, CO₂ emission into the atmosphere

could be reduced to 80.6% of the total CO₂ emitted from mushrooms during mushroom cultivation in this study.

This result is a method that can achieve a CO₂ reduction when construct the plant cultivation system. These studies can also be utilized in the life support systems research. From 2014, NASA has been trying to consume the CO₂ generated by astronauts and to supply fresh vegetables using small plant cultivation systems in the International Space Station (ISS) (Stutte et al., 2011; Zabel et al., 2014). If astronauts have to stay over a long period in the space, the life support systems require biological reproduction. In conclusion, the simultaneous cultivation system of lettuces and mushrooms designed in this experiment will reduce the CO₂ emission and improve the plant production.

LITERATURE CITED

- Daunicht, H.J. 1997. Gas turnover and gas conditions in hermetically closed plant production systems, pp. 225-244. In: Goto, E., K. Kurata, M. Hayashi, and S. Sase. (eds.). Plant production in closed ecosystems. Kluwer Academic Publishers, Dordrecht, The Netherlands.
- Gitelson, I.I., G.M. Lisovsky, and R.D. MacElroy. 2003. Manmade closed ecological systems. CRC press, London, UK. pp. 179-182.
- Hendrickx, L., H. de Wever, V. Hermans, F. Mastroleo, N. Morin, A. Wilmotte, P. Janssen, and M. Mergeay. 2006. Microbial ecology of the closed artificial ecosystem

- MELiSSA (Micro-Ecological Life Support System Alternative): Reinventing and compartmentalizing the Earth's food and oxygen regeneration system for long-haul space exploration missions. *Research in Microbiology*. 157: 77-86.
- Jang, M.J., T.M. Ha, Y.H. Lee, and Y.C. Ju. 2009. Growth characteristics of variety of oyster mushroom (*Pleurotus ostreatus*) as affected by number of air exchanges. *Journal of Bio-Environmental Control* 18: 208-214.
- Jung, D.H., C.K. Kim, K.H. Oh, D.H. Lee, M.S. Kim, J.H. Shin, and J.E. Son. 2014. Analyses of CO₂ concentration and balance in a closed production system for king oyster mushroom and lettuce. *Korean Journal of Horticultural Science and Technology* 10: 628-635.
- Kitaya, Y., A. Tani, M. Kiyota, and I. Aiga. 1994. Plant growth and gas balance in a plant and mushroom cultivation system. *Advanced Space Research* 14: 281-284.
- Leadley, P.W., P.A. Niklaus, and R. Stocker. 1999. A field study of the effects of elevated CO₂ on plant biomass and community structure in a calcareous grassland. *Oecologia* 118: 39-49.
- Ryu, J.S., M.K. Kim, S.H. Cho, Y.C. Yun, W.M. Seo, and H.S. Lee. 2005. Optimal CO₂ level for cultivation of *Pleurotus eryngii*. *Journal of Mushroom Science and Production* 3: 95-99.
- Son, J.E., J.S. Park, and H.Y. Park. 1999. Analysis of carbon dioxide changes in urban-type plant factory system. *Journal of Korean Society for Horticultural Science*. 40: 205-208.
- Stutte, G.W., G. Newsham, R.M. Morrow, and R.M. Wheeler. 2011. Concept for sustained

plant production on ISS using VEGGIE capillary mat rooting system. 44th International Conference on Environmental Systems, Portland, Oregon. AIAA Technology Paper 2011-5263.

Thavivongse, S., and M. Buppachat. 2013. Grey oyster mushroom for food security versus CO₂ emission. *Journal of Environmental Research and Development* 7: 1363-1368.

Volk, T., and J. D. Rummel. 1987. Mass balances for a biological life support system simulation model. *Advances in Space Research*. 7: 141-148.

Zabel, P., M. Bamsey, D. Schubert, and M. Tajmar. 2014. Review and analysis of plant growth chambers and greenhouse modules for space. 44th International Conference on Environmental Systems, Tucson, Arizona. ICES-2014-120.

Table III-1. Parameters used in the models.

Parameter	Description
V	Volume of the chamber (L)
$C_{L1} \sim C_{L3}$	CO ₂ concentration in the lettuce chambers ($\mu\text{mol}\cdot\text{mol}^{-1}$)
C_M	CO ₂ concentration in the mushroom chamber ($\mu\text{mol}\cdot\text{mol}^{-1}$)
C_X	CO ₂ concentration in the mixing chamber ($\mu\text{mol}\cdot\text{mol}^{-1}$)
C_O	CO ₂ concentration in the external air ($\mu\text{mol}\cdot\text{mol}^{-1}$)
$Q_{L1} \sim Q_{L3}$	Flow rate of the diaphragm pumps between lettuce and mixing chambers ($\text{L}\cdot\text{min}^{-1}$)
Q_M	Flow rate of the diaphragm pumps between mushroom and mixing chambers ($\text{L}\cdot\text{min}^{-1}$)
Q_X	Flow rate of the diaphragm pumps between mixing chamber and external air ($\text{L}\cdot\text{min}^{-1}$)
$LN1 \sim LN3$	Number of lettuces at particular growth stage
MN	Number of mushrooms at particular growth stage
$P1 \sim P3$	Accumulated photosynthetic rate in the each lettuce chambers ($\mu\text{molCO}_2\cdot\text{mol}^{-1}\cdot\text{s}^{-1}$)
R	Accumulated CO ₂ emission rate in the mushroom chamber ($\mu\text{molCO}_2\cdot\text{mol}^{-1}\cdot\text{s}^{-1}$)

Table III-2. Photoperiod in the lettuce chambers.

Period (h)	Chamber 1	Chamber 2	Chamber 3
00 : 00 ~ 08 : 00	Light	Light	Dark
08 : 00 ~ 16 : 00	Dark	Light	Light
16 : 00 ~ 00 : 00	Light	Dark	Light

Table III-3. Fresh weight and leaf area of the lettuces before and after experiments.

Growth stage (DAT ^z)	Before	After
	Shoot fresh weight (g)	
0	0.25±0.14 ^y a*	-
5	1.41±0.43ab	2.33±0.51ab
10	4.30±0.60bc	5.58±1.12c
15	10.10±1.35d	14.05±0.48e
20	25.07±2.91f	32.48±2.40g
25	54.58±1.99h	58.07±5.32i
	Leaf area (cm ²)	
0	11.37±2.37a	-
5	45.31±16.42a	74.37±10.04ab
10	147.20±16.36bc	165.26±17.30c
15	331.50±38.34d	414.37±16.89e
20	693.61±83.64f	935.55±104.78g
25	1510.88±74.20h	1533.15±84.23h

*Different letters indicate statistically significant differences (ANOVA/Duncan) ($P < 0.05$)

^zDays after transplanting.

^yMean±SD (n = 6).

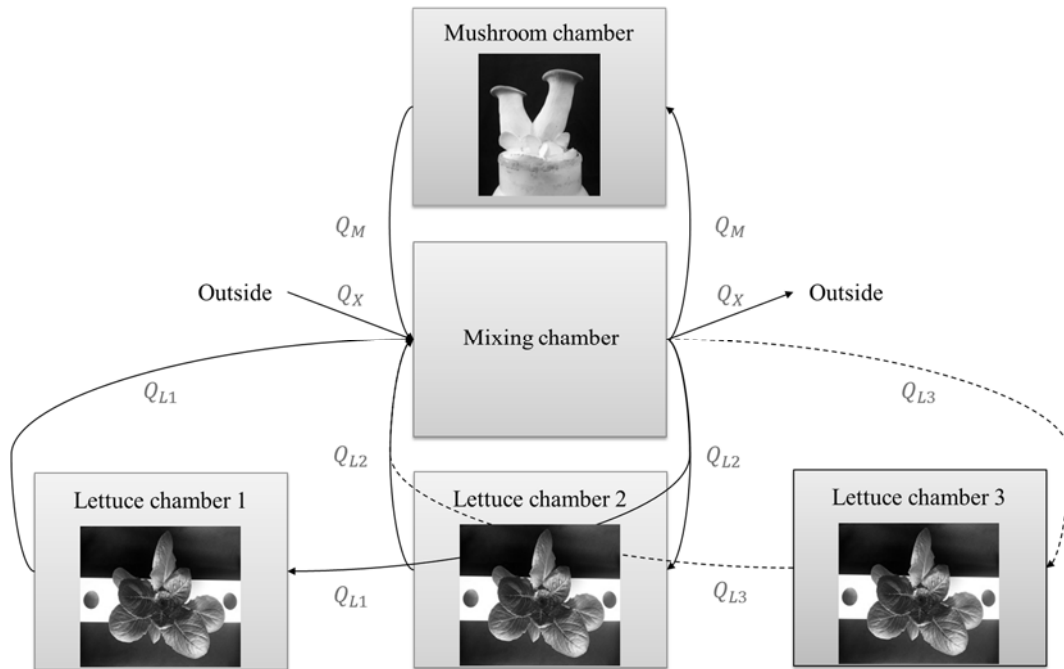


Fig. III-1. Conceptual diagram of a system consisting of three lettuce chambers, one mushroom chamber, and one CO₂ mixing chamber. Arrow and symbol mean air flow air flow rate, respectively. Solid and dashed arrows mean pump-on and off, respectively.

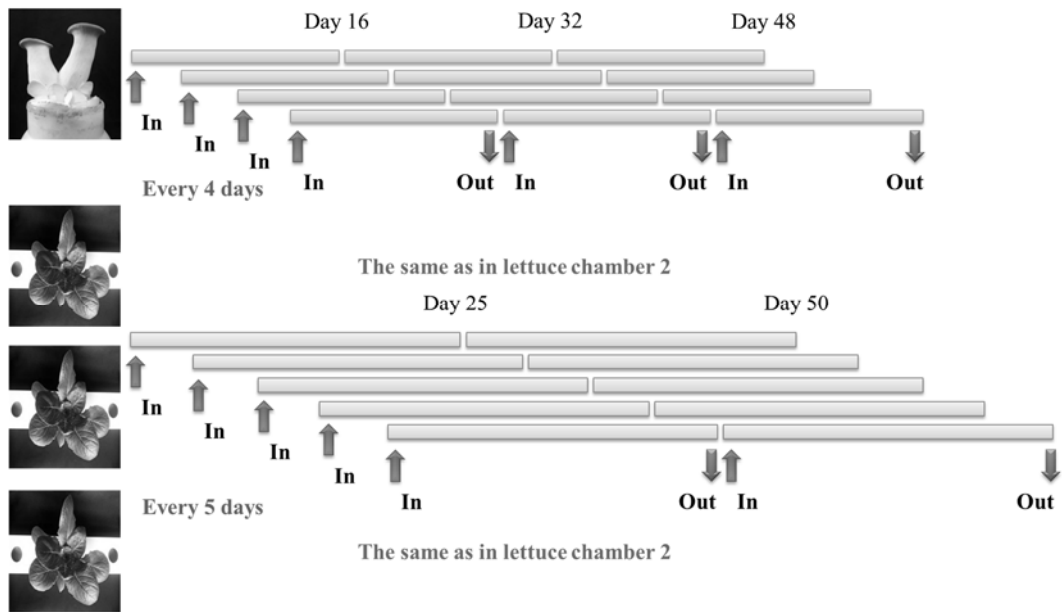


Fig. III-2. Schematic diagram of the continuous cultivation. Three bottles of new mushrooms put into the chamber every 4 days and three lettuces into each chamber every 5 days. Total number of lettuces and mushrooms in each chamber at a certain time are 15 and 12, respectively.

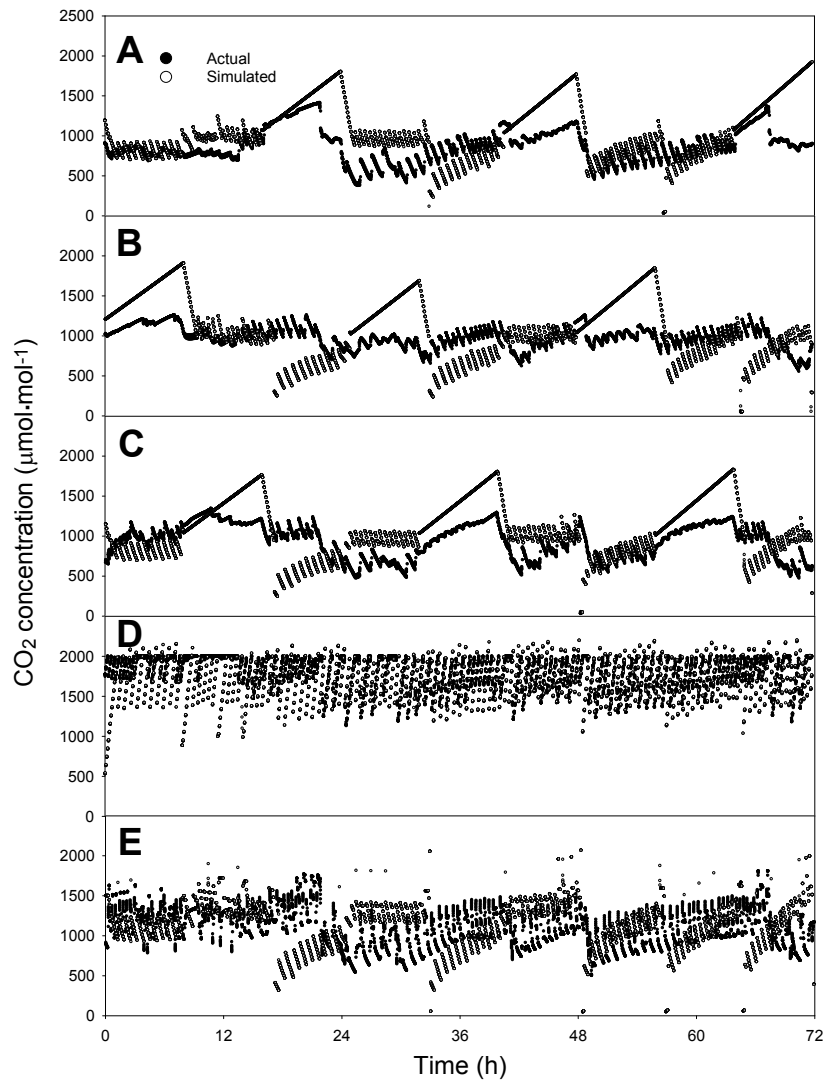


Fig. III-3. Actual and simulated CO₂ concentrations in each chamber for 3 days; lettuce chamber 1 (A), lettuce chamber 2 (B), lettuce chamber 3 (C), mushroom chamber (D), and mixing chamber (E). Solid and void circles mean the actual and simulated CO₂ concentrations.

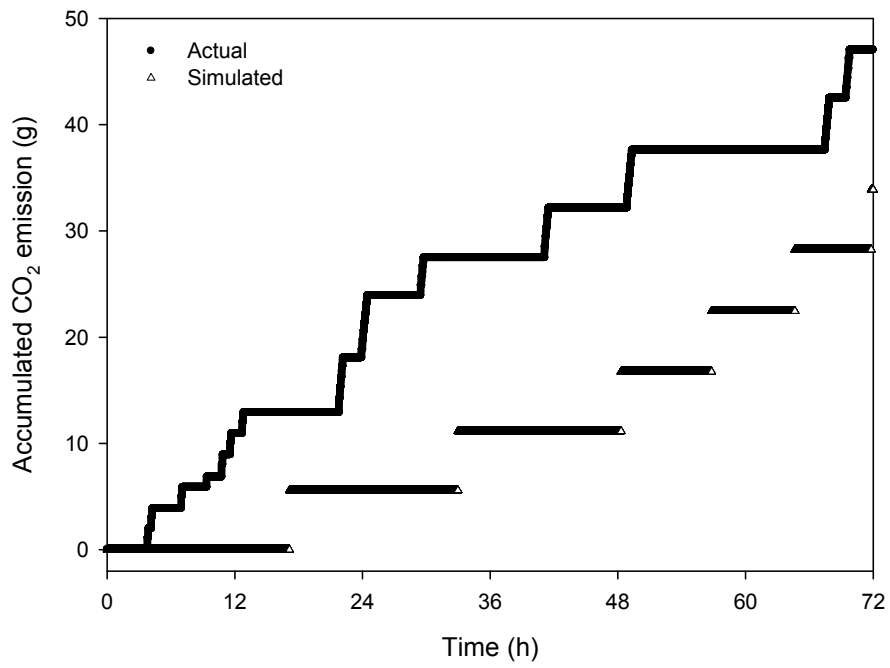


Fig. III-3. Accumulated CO₂ emission into the atmosphere for 3 days. Solid and void circles mean the actual simulated CO₂ emissions.

CONCLUSION

The CO₂ emission rate models of mushrooms before and after thinning were developed as Eqs. I-11 and I-12, respectively. The CO₂ emission models showed good agreements with measured data. And it is possible to estimate the increase in CO₂ concentration in the mushroom cultivation facilities. Also the photosynthetic rate models of lettuces were developed as Eqs. II-7 and II-8. Thornley's dynamic model for photosynthesis was used to express the canopy photosynthesis because this model reflects physiological reactions of plants well. Using simulation methods, CO₂ concentrations in the lettuce and mushroom chambers could be accurately estimated in the simultaneous cultivation and enabled to design the efficient cultivation systems. CO₂ concentrations in the lettuce and mushroom chambers were verified and shown to be controlled within allowable ranges. With the simultaneous cultivation system, CO₂ emission into the atmosphere could be reduced to 80.6% of the total CO₂ emitted from mushrooms by respiration. Because CO₂ is one of the factors responsible for global warming, development of the methods to minimize CO₂ emission will be useful for mushroom cultivation. These studies can also be utilized to the life support systems in which reuse the CO₂ caused by the crew for photosynthesis of crops. In conclusion, the simultaneous cultivation system of lettuces and mushrooms designed in this experiment enables to reduce the CO₂ emission as well as improve the plant production.

APPENDICES

Simulation Codes for Lettuce and Mushroom Simultaneous Cultivation

```
clear all
clc

% Time unit (5 second), simulation for 3 days

STARTTIME = 0;
STOPTIME = 51840;
DT = 1;
Duration = (STOPTIME - STARTTIME)/DT + 1;

% Used variables

P1(Duration,1) = 0;
P2(Duration,1) = 0;
P3(Duration,1) = 0;
R(Duration,1) = 0;

P11(Duration,1) = 0;
P21(Duration,1) = 0;
P31(Duration,1) = 0;

P12(Duration,1) = 0;
P22(Duration,1) = 0;
P32(Duration,1) = 0;

P13(Duration,1) = 0;
P23(Duration,1) = 0;
P33(Duration,1) = 0;

P14(Duration,1) = 0;
P24(Duration,1) = 0;
P34(Duration,1) = 0;

P15(Duration,1) = 0;
P25(Duration,1) = 0;
P35(Duration,1) = 0;

R1(Duration,1) = 0;
R2(Duration,1) = 0;
```

```

R3(Duration,1) = 0;
R4(Duration,1) = 0;

CL1(Duration,1) = 0;
CL2(Duration,1) = 0;
CL3(Duration,1) = 0;
CM(Duration,1) = 0;
CX(Duration,1) = 0;

CL1(1,1) = 1200;
CL2(1,1) = 1200;
CL3(1,1) = 1200;
CM(1,1) = 500;
CX(1,1) = 1500;

QL1I(Duration,1) = 0;
QL1O(Duration,1) = 0;
QL2I(Duration,1) = 0;
QL2O(Duration,1) = 0;
QL3I(Duration,1) = 0;
QL3O(Duration,1) = 0;
QMI(Duration,1) = 0;
QMO(Duration,1) = 0;
VXI(Duration,1) = 0;
VXO(Duration,1) = 0;

LN1(Duration,1) = 3;
LN1(1,1) = 3;
LN2(Duration,1) = 3;
LN2(1,1) = 3;
LN3(Duration,1) = 3;
LN3(1,1) = 3;

MN(Duration,1) = 3;
MN(1,1) = 3;

COE(Duration,1) = 0;
COE(1,1) = 0;

COEV(Duration,1) = 0;
COEV(1,1) = 0;

CO = 500;

TIME = (STARTTIME:DT:STOPTIME)';

% Iteration start

```

```

for time = STARTTIME+1:STOPTIME/DT-1

    % Timer for mushroom, lettuce and pumps

    ClockM = mod(time, 276480);

    ClockL1 = mod(time, 17280);
    ClockL2 = mod(time-5760, 17280);
    ClockL3 = mod(time-11520, 17280);

    LI840Clock = mod(time, 120);

    % Lettuce Photosynthesis Set 1

    if (ClockL1 <= 11520)
        P11(time,1) = 5*(((21.812*exp(-0.107*(mod(time,
432000)/17280))*(0.735502*CL1(time, 1)))/(57.4*exp(-
0.057*(mod(time, 432000)/17280))+0.38*exp(-0.05*(mod(time,
432000)/17280))*(0.735502*CL1(time, 1))))-18.608*exp(-
0.056*(mod(time, 432000)/17280)))*0.0064755*exp(0.132*(mod(time,
432000)/17280))*44*0.000553846;
    else
        P11(time,1) = -5*4.735*exp(-0.065*(mod(time,
432000)/17280))*0.0064755*exp(0.132*(mod(time,
432000)/17280))*44*0.000553846;
    end

    if (ClockL2 <= 11520)
        P21(time,1) = 5*(((21.812*exp(-0.107*(mod(time,
432000)/17280))*(0.735502*CL2(time, 1)))/(57.4*exp(-
0.057*(mod(time, 432000)/17280))+0.38*exp(-0.05*(mod(time,
432000)/17280))*(0.735502*CL2(time, 1))))-18.608*exp(-
0.056*(mod(time, 432000)/17280)))*0.0064755*exp(0.132*(mod(time,
432000)/17280))*44*0.000553846;
    else
        P21(time,1) = -5*4.735*exp(-0.065*(mod(time,
432000)/17280))*0.0064755*exp(0.132*(mod(time,
432000)/17280))*44*0.000553846;
    end

    if (ClockL3 <= 11520)
        P31(time,1) = 5*(((21.812*exp(-0.107*(mod(time,
432000)/17280))*(0.735502*CL3(time, 1)))/(57.4*exp(-
0.057*(mod(time, 432000)/17280))+0.38*exp(-0.05*(mod(time,
432000)/17280))*(0.735502*CL3(time, 1))))-18.608*exp(-
0.056*(mod(time, 432000)/17280)))*0.0064755*exp(0.132*(mod(time,

```

```

432000)/17280))*44*0.000553846;
else
    P31(time,1) = -5*4.735*exp(-0.065*(mod(time,
432000)/17280))*0.0064755*exp(0.132*(mod(time,
432000)/17280))*44*0.000553846;
end

% Lettuce Photosynthesis Set 2

if (ClockL1 <= 11520)
    P12(time,1) = 5*(((21.812*exp(-0.107*(mod(time-86400,
432000)/17280))*(0.735502*CL1(time, 1)))/(57.4*exp(-
0.057*(mod(time-86400, 432000)/17280))+0.38*exp(-0.05*(mod(time-
86400, 432000)/17280))*(0.735502*CL1(time, 1))))-18.608*exp(-
0.056*(mod(time-86400,
432000)/17280)))*0.0064755*exp(0.132*(mod(time-86400,
432000)/17280))*44*0.000553846;
else
    P12(time,1) = -5*4.735*exp(-0.065*(mod(time-86400,
432000)/17280))*0.0064755*exp(0.132*(mod(time-86400,
432000)/17280))*44*0.000553846;
end

if (ClockL2 <= 11520)
    P22(time,1) = 5*(((21.812*exp(-0.107*(mod(time-86400,
432000)/17280))*(0.735502*CL2(time, 1)))/(57.4*exp(-
0.057*(mod(time-86400, 432000)/17280))+0.38*exp(-0.05*(mod(time-
86400, 432000)/17280))*(0.735502*CL2(time, 1))))-18.608*exp(-
0.056*(mod(time-86400,
432000)/17280)))*0.0064755*exp(0.132*(mod(time-86400,
432000)/17280))*44*0.000553846;
else
    P22(time,1) = -5*4.735*exp(-0.065*(mod(time-86400,
432000)/17280))*0.0064755*exp(0.132*(mod(time-86400,
432000)/17280))*44*0.000553846;
end

if (ClockL3 <= 11520)
    P32(time,1) = 5*(((21.812*exp(-0.107*(mod(time-86400,
432000)/17280))*(0.735502*CL3(time, 1)))/(57.4*exp(-
0.057*(mod(time-86400, 432000)/17280))+0.38*exp(-0.05*(mod(time-
86400, 432000)/17280))*(0.735502*CL3(time, 1))))-18.608*exp(-
0.056*(mod(time-86400,
432000)/17280)))*0.0064755*exp(0.132*(mod(time-86400,
432000)/17280))*44*0.000553846;
else
    P32(time,1) = -5*4.735*exp(-0.065*(mod(time-86400,
432000)/17280))*0.0064755*exp(0.132*(mod(time-86400,

```

```

432000)/17280))*44*0.000553846;
end

% Lettuce Photosynthesis Set 3

if (ClockL1 <= 11520)
    P13(time,1) = 5*(((21.812*exp(-0.107*(mod(time-172800,
432000)/17280))*(0.735502*CL1(time, 1)))/(57.4*exp(-
0.057*(mod(time-172800, 432000)/17280))+0.38*exp(-0.05*(mod(time-
172800, 432000)/17280))*(0.735502*CL1(time, 1))))-18.608*exp(-
0.056*(mod(time-172800,
432000)/17280)))*0.0064755*exp(0.132*(mod(time-172800,
432000)/17280))*44*0.000553846;
else
    P13(time,1) = -5*4.735*exp(-0.065*(mod(time-172800,
432000)/17280))*0.0064755*exp(0.132*(mod(time-172800,
432000)/17280))*44*0.000553846;
end

if (ClockL2 <= 11520)
    P23(time,1) = 5*(((21.812*exp(-0.107*(mod(time-172800,
432000)/17280))*(0.735502*CL2(time, 1)))/(57.4*exp(-
0.057*(mod(time-172800, 432000)/17280))+0.38*exp(-0.05*(mod(time-
172800, 432000)/17280))*(0.735502*CL2(time, 1))))-18.608*exp(-
0.056*(mod(time-172800,
432000)/17280)))*0.0064755*exp(0.132*(mod(time-172800,
432000)/17280))*44*0.000553846;
else
    P23(time,1) = -5*4.735*exp(-0.065*(mod(time-172800,
432000)/17280))*0.0064755*exp(0.132*(mod(time-172800,
432000)/17280))*44*0.000553846;
end

if (ClockL3 <= 11520)
    P33(time,1) = 5*(((21.812*exp(-0.107*(mod(time-172800,
432000)/17280))*(0.735502*CL3(time, 1)))/(57.4*exp(-
0.057*(mod(time-172800, 432000)/17280))+0.38*exp(-0.05*(mod(time-
172800, 432000)/17280))*(0.735502*CL3(time, 1))))-18.608*exp(-
0.056*(mod(time-172800,
432000)/17280)))*0.0064755*exp(0.132*(mod(time-172800,
432000)/17280))*44*0.000553846;
else
    P33(time,1) = -5*4.735*exp(-0.065*(mod(time-172800,
432000)/17280))*0.0064755*exp(0.132*(mod(time-172800,
432000)/17280))*44*0.000553846;
end

% Lettuce Photosynthesis Set 4

```

```

    if (ClockL1 <= 11520)
        P14(time,1) = 5*(((21.812*exp(-0.107*(mod(time-259200,
432000)/17280))*(0.735502*CL1(time, 1)))/(57.4*exp(-
0.057*(mod(time-259200, 432000)/17280))+0.38*exp(-0.05*(mod(time-
259200, 432000)/17280))*(0.735502*CL1(time, 1))))-18.608*exp(-
0.056*(mod(time-259200,
432000)/17280)))*0.0064755*exp(0.132*(mod(time-259200,
432000)/17280))*44*0.000553846;
    else
        P14(time,1) = -5*4.735*exp(-0.065*(mod(time-259200,
432000)/17280))*0.0064755*exp(0.132*(mod(time-259200,
432000)/17280))*44*0.000553846;
    end

    if (ClockL2 <= 11520)
        P24(time,1) = 5*(((21.812*exp(-0.107*(mod(time-259200,
432000)/17280))*(0.735502*CL2(time, 1)))/(57.4*exp(-
0.057*(mod(time-259200, 432000)/17280))+0.38*exp(-0.05*(mod(time-
259200, 432000)/17280))*(0.735502*CL2(time, 1))))-18.608*exp(-
0.056*(mod(time-259200,
432000)/17280)))*0.0064755*exp(0.132*(mod(time-259200,
432000)/17280))*44*0.000553846;
    else
        P24(time,1) = -5*4.735*exp(-0.065*(mod(time-259200,
432000)/17280))*0.0064755*exp(0.132*(mod(time-259200,
432000)/17280))*44*0.000553846;
    end

    if (ClockL3 <= 11520)
        P34(time,1) = 5*(((21.812*exp(-0.107*(mod(time-259200,
432000)/17280))*(0.735502*CL3(time, 1)))/(57.4*exp(-
0.057*(mod(time-259200, 432000)/17280))+0.38*exp(-0.05*(mod(time-
259200, 432000)/17280))*(0.735502*CL3(time, 1))))-18.608*exp(-
0.056*(mod(time-259200,
432000)/17280)))*0.0064755*exp(0.132*(mod(time-259200,
432000)/17280))*44*0.000553846;
    else
        P34(time,1) = -5*4.735*exp(-0.065*(mod(time-259200,
432000)/17280))*0.0064755*exp(0.132*(mod(time-259200,
432000)/17280))*44*0.000553846;
    end

    % Lettuce Photosynthesis Set 5

    if (ClockL1 <= 11520)
        P15(time,1) = 5*(((21.812*exp(-0.107*(mod(time-345600,
432000)/17280))*(0.735502*CL1(time, 1)))/(57.4*exp(-

```

```

0.057*(mod(time-345600, 432000)/17280))+0.38*exp(-0.05*(mod(time-
345600, 432000)/17280))*(0.735502*CL1(time, 1)))-18.608*exp(-
0.056*(mod(time-345600,
432000)/17280))*0.0064755*exp(0.132*(mod(time-345600,
432000)/17280))*44*0.000553846;
else
P15(time,1) = -5*4.735*exp(-0.065*(mod(time-345600,
432000)/17280))*0.0064755*exp(0.132*(mod(time-345600,
432000)/17280))*44*0.000553846;
end

if (ClockL2 <= 11520)
P25(time,1) = 5*(((21.812*exp(-0.107*(mod(time-345600,
432000)/17280))*(0.735502*CL2(time, 1)))/(57.4*exp(-
0.057*(mod(time-345600, 432000)/17280))+0.38*exp(-0.05*(mod(time-
345600, 432000)/17280))*(0.735502*CL2(time, 1)))-18.608*exp(-
0.056*(mod(time-345600,
432000)/17280))*0.0064755*exp(0.132*(mod(time-345600,
432000)/17280))*44*0.000553846;
else
P25(time,1) = -5*4.735*exp(-0.065*(mod(time-345600,
432000)/17280))*0.0064755*exp(0.132*(mod(time-345600,
432000)/17280))*44*0.000553846;
end

if (ClockL3 <= 11520)
P35(time,1) = 5*(((21.812*exp(-0.107*(mod(time-345600,
432000)/17280))*(0.735502*CL3(time, 1)))/(57.4*exp(-
0.057*(mod(time-345600, 432000)/17280))+0.38*exp(-0.05*(mod(time-
345600, 432000)/17280))*(0.735502*CL3(time, 1)))-18.608*exp(-
0.056*(mod(time-345600,
432000)/17280))*0.0064755*exp(0.132*(mod(time-345600,
432000)/17280))*44*0.000553846;
else
P35(time,1) = -5*4.735*exp(-0.065*(mod(time-345600,
432000)/17280))*0.0064755*exp(0.132*(mod(time-345600,
432000)/17280))*44*0.000553846;
end

% Mushroom Respiration Set 1

if (ClockM <= 207360)
R1(time,1) = 5*(0.0191365*exp(0.549*mod(time-51840,
276480)/17280)+43.5288)*0.000538928;
else
R1(time,1) = 5*(0.0061971*exp(0.549*mod(time-51840,
276480)/17280)+62.0868)*0.000538928;
end

```

```

% Mushroom Respiration Set 2

if (ClockM <= 207360)
    R2(time,1) = 5*(0.0191365*exp(0.549*mod(time-120960,
276480)/17280)+43.5288)*0.000538928;
else
    R2(time,1) = 5*(0.0061971*exp(0.549*mod(time-120960,
276480)/17280)+62.0868)*0.000538928;
end

% Mushroom Respiration Set 3

if (ClockM <= 207360)
    R3(time,1) = 5*(0.0191365*exp(0.549*mod(time-190080,
276480)/17280)+43.5288)*0.000538928;
else
    R3(time,1) = 5*(0.0061971*exp(0.549*mod(time-190080,
276480)/17280)+62.0868)*0.000538928;
end

% Mushroom Respiration Set 4

if (ClockM <= 207360)
    R4(time,1) = 5*(0.0191365*exp(0.549*mod(time-259200,
276480)/17280)+43.5288)*0.000538928;
else
    R4(time,1) = 5*(0.0061971*exp(0.549*mod(time-259200,
276480)/17280)+62.0868)*0.000538928;
end

% Differential equation solving (Using Euler's method)

CL1(time + 1,1) = CL1(time,1) + DT*(CX(time,1)*QL1I(time,1) -
CL1(time,1)*QL1O(time,1) - LN1(time,1)*(P11(time,1) + P12(time,1)
+ P13(time,1) + P14(time,1) + P15(time,1)));

CL2(time + 1,1) = CL2(time,1) + DT*(CX(time,1)*QL2I(time,1) -
CL2(time,1)*QL2O(time,1) - LN2(time,1)*(P21(time,1) + P22(time,1)
+ P23(time,1) + P24(time,1) + P25(time,1)));

CL3(time + 1,1) = CL3(time,1) + DT*(CX(time,1)*QL3I(time,1) -
CL3(time,1)*QL3O(time,1) - LN3(time,1)*(P31(time,1) + P32(time,1)
+ P33(time,1) + P34(time,1) + P35(time,1)));

CM(time + 1,1) = CM(time,1) + DT*(CX(time,1)*QMI(time,1) -
CM(time,1)*QMO(time,1) + MN(time,1)*(R1(time,1) + R2(time,1) +

```

```

R3(time,1) + R4(time,1));

CX(time + 1,1) = CX(time,1) + DT*(CL1(time,1)*QL1O(time,1) +
CL2(time,1)*QL2O(time,1) + CL3(time,1)*QL3O(time,1) +
CM(time,1)*QMO(time,1) - CX(time,1)*QL1I(time,1) -
CX(time,1)*QL2I(time,1) - CX(time,1)*QL3I(time,1) -
CX(time,1)*QMI(time,1) - CX(time,1)*VXO(time,1) + CO*VXI(time,1));

COE(time + 1,1) = COE(time, 1) +
DT*(CX(time,1)*0.00180555*VXO(time,1));

COEV(time + 1,1) = (CX(time, 1)*0.00180555/125)*VXO(time, 1);

% Fan ON/OFF Conditions

if(LI840Clock >= 0 && LI840Clock < 24)
    if(CL1(time+1,1) <= 1000)
        QL1I(time+1,1) = 0.3;
    elseif(CL1(time+1,1) > 1000 && abs(CL1(time+1,1) -
CL1(time,1)) < 0.01)
        QL1I(time+1,1) = 0;
    end
else
    QL1I(time+1,1) = QL1I(time,1);
end

if(LI840Clock >= 0 && LI840Clock < 24)
    if(CL1(time+1,1) <= 1000)
        QL1O(time+1,1) = 0.4;
    elseif(CL1(time+1,1) > 1000 && abs(CL1(time+1,1) -
CL1(time,1)) < 0.01)
        QL1O(time+1,1) = 0;
    end
else
    QL1O(time+1,1) = QL1O(time,1);
end

if(LI840Clock >= 24 && LI840Clock < 48)
    if(CL2(time+1,1) <= 1000)
        QL2I(time+1,1) = 0.3;
    elseif(CL2(time+1,1) > 1000 && abs(CL2(time+1,1) -
CL2(time,1)) < 0.01)
        QL2I(time+1,1) = 0;
    end
end

```

```

else
    QL2I(time+1,1) = QL2I(time,1);
end

if(LI840Clock >= 24 && LI840Clock < 48)
    if(CL2(time+1,1) <= 1000)
        QL2O(time+1,1) = 0.4;
    elseif(CL2(time+1,1) > 1000 && abs(CL2(time+1,1) -
CL2(time,1)) < 0.01)
        QL2O(time+1,1) = 0;
    end
else
    QL2O(time+1,1) = QL2O(time,1);
end

if(LI840Clock >= 48 && LI840Clock < 72)
    if(CL3(time+1,1) <= 1000)
        QL3I(time+1,1) = 0.3;
    elseif(CL3(time+1,1) > 1000 && abs(CL3(time+1,1) -
CL3(time,1)) < 0.01)
        QL3I(time+1,1) = 0;
    end
else
    QL3I(time+1,1) = QL3I(time,1);
end

if(LI840Clock >= 48 && LI840Clock < 72)
    if(CL3(time+1,1) <= 1000)
        QL3O(time+1,1) = 0.4;
    elseif(CL3(time+1,1) > 1000 && abs(CL3(time+1,1) -
CL3(time,1)) < 0.01)
        QL3O(time+1,1) = 0;
    end
else
    QL3O(time+1,1) = QL3O(time,1);
end

if(LI840Clock >= 72 && LI840Clock < 96)
    if (CM(time+1,1) >= 2000)
        QMI(time+1,1) = 0.3;
    elseif(CM(time+1,1) < 2000 && abs(CM(time+1,1) -
CM(time,1)) < 0.1)
        QMI(time+1,1) = 0;
    end
else
    QMI(time+1,1) = QMI(time,1);
end

```

```

end

if(LI840Clock >= 72 && LI840Clock < 96)
    if (CM(time+1,1) >= 2000)
        QMO(time+1,1) = 0.5;
    elseif(CM(time+1,1) < 2000 && abs(CM(time+1,1) -
CM(time,1)) < 0.1)
        QMO(time+1,1) = 0;
    end
else
    QMO(time+1,1) = QMO(time,1);
end

if(LI840Clock >= 96 && LI840Clock < 120)
    if (CX(time+1,1) >= 2000)
        VXI(time+1,1) = 0.4;
    elseif(CX(time+1,1) < 2000 && abs(CX(time+1,1) -
CX(time,1)) < 0.1)
        VXI(time+1,1) = 0;
    end
else
    VXI(time+1,1) = VXI(time,1);
end

if(LI840Clock >= 96 && LI840Clock < 120)
    if (CX(time+1,1) >= 2000)
        VXO(time+1,1) = 1.5;
    elseif(CX(time+1,1) < 2000 && abs(CX(time+1,1) -
CX(time,1)) < 0.1)
        VXO(time+1,1) = 0;
    end
else
    VXO(time+1,1) = VXO(time,1);
end

% Number of mushrooms and lettuces

LN1(time+1,1) = LN1(time,1);
LN2(time+1,1) = LN2(time,1);
LN3(time+1,1) = LN3(time,1);
MN(time+1,1) = MN(time,1);

% Photosynthesis and Respiration in each chambers

```

```

P1(time,1) = (P11(time,1)/(0.0064755*exp(0.132*(mod(time,
432000)/17280))*44*0.000553846) +
P12(time,1)/(0.0064755*exp(0.132*(mod(time-86400,
432000)/17280))*44*0.000553846) +
P13(time,1)/(0.0064755*exp(0.132*(mod(time-172800,
432000)/17280))*44*0.000553846) +
P14(time,1)/(0.0064755*exp(0.132*(mod(time-259200,
432000)/17280))*44*0.000553846) +
P15(time,1)/(0.0064755*exp(0.132*(mod(time-345600,
432000)/17280))*44*0.000553846));
P2(time,1) = (P21(time,1)/(0.0064755*exp(0.132*(mod(time,
432000)/17280))*44*0.000553846) +
P22(time,1)/(0.0064755*exp(0.132*(mod(time-86400,
432000)/17280))*44*0.000553846) +
P23(time,1)/(0.0064755*exp(0.132*(mod(time-172800,
432000)/17280))*44*0.000553846) +
P24(time,1)/(0.0064755*exp(0.132*(mod(time-259200,
432000)/17280))*44*0.000553846) +
P25(time,1)/(0.0064755*exp(0.132*(mod(time-345600,
432000)/17280))*44*0.000553846));
P3(time,1) = (P31(time,1)/(0.0064755*exp(0.132*(mod(time,
432000)/17280))*44*0.000553846) +
P32(time,1)/(0.0064755*exp(0.132*(mod(time-86400,
432000)/17280))*44*0.000553846) +
P33(time,1)/(0.0064755*exp(0.132*(mod(time-172800,
432000)/17280))*44*0.000553846) +
P34(time,1)/(0.0064755*exp(0.132*(mod(time-259200,
432000)/17280))*44*0.000553846) +
P35(time,1)/(0.0064755*exp(0.132*(mod(time-345600,
432000)/17280))*44*0.000553846));
R(time,1) = (R1(time,1) + R2(time,1) + R3(time,1) +
R4(time,1))/0.00184278;

```

```
end
```

```
% Plotting graphs
```

```
figure;
plot(TIME,CL1,TIME,CL2,TIME,CL3,TIME,CM,TIME,CX);
```

```
figure;
plot(TIME,COE);
```

Simulation Codes for Mushroom Only Cultivation

```
clear all
clc

% Time unit (5 second), simulation for 3 days

STARTTIME = 0;
STOPTIME = 51840;
DT = 1;
Duration = (STOPTIME - STARTTIME)/DT + 1;

% Used variables

R(Duration,1) = 0;

R1(Duration,1) = 0;
R2(Duration,1) = 0;
R3(Duration,1) = 0;
R4(Duration,1) = 0;

CM(Duration,1) = 0;
CM(1,1) = 500;

VXI(Duration,1) = 0;
VXO(Duration,1) = 0;

MN(Duration,1) = 3;
MN(1,1) = 3;

COE(Duration,1) = 0;
COE(1,1) = 0;

COEV(Duration,1) = 0;
COEV(1,1) = 0;

CO(Duration,1) = 500;

TIME = (STARTTIME:DT:STOPTIME)';

% Iteration start

for time = STARTTIME+1:STOPTIME/DT-1
```

```

% Timer for mushroom, lettuce and pumps

ClockM = mod(time, 276480);

LI840Clock = mod(time, 120);

% Mushroom Respiration Set 1

if (ClockM <= 207360)
    R1(time,1) = 5*(0.0191365*exp(0.549*mod(time-51840,
276480)/17280)+43.5288)*0.000538928;
else
    R1(time,1) = 5*(0.0061971*exp(0.549*mod(time-51840,
276480)/17280)+62.0868)*0.000538928;
end

% Mushroom Respiration Set 2

if (ClockM <= 207360)
    R2(time,1) = 5*(0.0191365*exp(0.549*mod(time-120960,
276480)/17280)+43.5288)*0.000538928;
else
    R2(time,1) = 5*(0.0061971*exp(0.549*mod(time-120960,
276480)/17280)+62.0868)*0.000538928;
end

% Mushroom Respiration Set 3

if (ClockM <= 207360)
    R3(time,1) = 5*(0.0191365*exp(0.549*mod(time-190080,
276480)/17280)+43.5288)*0.000538928;
else
    R3(time,1) = 5*(0.0061971*exp(0.549*mod(time-190080,
276480)/17280)+62.0868)*0.000538928;
end

% Mushroom Respiration Set 4

if (ClockM <= 207360)
    R4(time,1) = 5*(0.0191365*exp(0.549*mod(time-259200,
276480)/17280)+43.5288)*0.000538928;
else
    R4(time,1) = 5*(0.0061971*exp(0.549*mod(time-259200,
276480)/17280)+62.0868)*0.000538928;
end

```

```

% Differential equation solving (Using Euler's method)

CM(time + 1,1) = CM(time,1) + DT*(CO(time,1)*VXI(time,1) -
CM(time,1)*VXO(time,1) + MN(time,1)*(R1(time,1) + R2(time,1) +
R3(time,1) + R4(time,1)));

COE(time + 1,1) = COE(time, 1) +
DT*(CM(time,1)*0.00180555*VXO(time,1));

COEV(time + 1,1) = (CM(time, 1)*0.00180555/125)*VXO(time, 1);

% Fan ON/OFF Conditions

if (CM(time+1,1) >= 2000)
    VXI(time+1,1) = 62/400;
elseif(CM(time+1,1) < 2000 && abs(CM(time+1,1) - CM(time,1)) <
3000)
    VXI(time+1,1) = 0;
end

if (CM(time+1,1) >= 2000)
    VXO(time+1,1) = 62/400;
elseif(CM(time+1,1) < 2000 && abs(CM(time+1,1) - CM(time,1)) <
3000)
    VXO(time+1,1) = 0;
end

% Number of mushrooms and lettuces

MN(time+1,1) = MN(time,1);
CO(time+1,1) = CO(time,1);

% Photosynthesis and Respiration in each chambers

R(time,1) = (R1(time,1) + R2(time,1) + R3(time,1) +
R4(time,1))/0.00184278;

```

```
end

% Plotting graphs

figure;
plot(TIME,CM);

figure;
plot(TIME,COE);
```

ABSTRACT IN KOREAN

최근 생명지원시스템에 대한 연구가 활발히 이루어지고 있지만, 다양한 내부 구성요소들이 상호작용하고 있기 때문에 실제로 실험을 수행하여 연구하기가 어렵다. 따라서 모델링과 시뮬레이션 방식을 이용한 생명지원시스템 연구가 점차 증가하고 있다. 버섯과 상추를 동시에 재배하여 버섯에서 발생한 CO₂ 를 상추에 시비하는 개념은 생명지원시스템 연구와 작물 생산 연구 양쪽에서 중요한 역할을 한다. 본 연구에서는 버섯의 호흡에 의해 발생하는 CO₂ 의 양과 상추가 광합성을 통해 소모하는 CO₂ 의 양을 정량화 하여 모델을 확립하고, 두 작물을 밀폐형 생산시스템에서 동시에 재배하는 경우 내부의 CO₂ 농도를 지속 가능한 재배를 위한 수준에서 유지할 수 있도록 하는 재배 전략을 확립하는 것을 목적으로 하였다. 버섯의 CO₂ 발생 속도와 상추의 광합성 속도는 밀폐형 아크릴 챔버를 이용하여 측정하였으며, 통계 프로그램을 이용하여 모델의 계수를 확정하였다. 확립된 모델을 이용하여 상추와 버섯을 동시에 재배하는 시스템을 구성하고 시뮬레이션하여 각 재배 챔버 내부의 CO₂ 농도 변화를 예측하였다. 또한 실증 실험을 수행하여 시뮬레이션과 비교하여 어떤 차이가 있는 지 알아보았다. 버섯의 CO₂ 발생 속도 모델과 상추의 광합성 속도 모델은 각각 R² 값이 0.642 와 0.939 로 높은 신뢰성을 보였다. 상추와 버섯을 동시에 재배하는 시스템에서 시뮬레이션과 실증 실험 모두 각 챔버 내부의 CO₂ 농도가 설정치 안에서 제어되는 것을 확인하였다. 또한 버섯을 단독으로 재배하는 것에 비해 대기 중으로 방출되는 누적 CO₂ 양이 80.6% 감소하는 것을 확인하였다. 이러한 연구를 바탕으로 각 작물 재배 시 CO₂ 농도를 제어할 수 있으며,

버섯 재배 시 대기 중으로 방출되는 CO₂의 양을 줄일 수 있을 것이다. 최종적으로 생명지원시스템 연구 분야에서도 기체 순환 전략을 확립하는 데 도움이 될 것이다.

주요어: 밀폐형 생산시스템, 버섯 호흡, 상추 균락 광합성, 이산화탄소 교환, 이산화탄소 모델

학번: 2014-20016